JOURNAL OF VIROLOGY, July 2009, p. 7305–7321 Vol. 83, No. 14
0022-538X/09/$08.00+0 doi:10.1128/JVI.02207-08

Induction of Robust Cellular and Humoral Virus-Specific Adaptive Immune Responses in Human Immunodeficiency Virus-Infected Humanized BLT Mice[▽]

Diana M. Brainard,[1,2] Edward Seung,[1] Nicole Frahm,[2,3] Annaiah Cariappa,[4] Charles C. Bailey,[5] William K. Hart,[1] Hae-Sook Shin,[1] Sarah F. Brooks,[1] Heather L. Knight,[2] Quentin Eichbaum,[2] Yong-Guang Yang,[6] Megan Sykes,[6] Bruce D. Walker,[2] Gordon J. Freeman,[7] Shiv Pillai,[4] Susan V. Westmoreland,[5] Christian Brander,[2,8,9] Andrew D. Luster,[1]†* and Andrew M. Tager[1]†*

Center for Immunology and Inflammatory Diseases, Division of Rheumatology, Allergy and Immunology, Massachusetts General Hospital, Harvard Medical School, Charlestown, Massachusetts 02129[1]; Ragon Institute of MGH, MIT, and Harvard and Division of AIDS, Harvard Medical School, Charlestown, Massachusetts 02129[2]; Vaccine and Infectious Disease Institute, Fred Hutchinson Cancer Research Center, Seattle, Washington 98109[3]; Center for Cancer Research, Massachusetts General Hospital, Harvard Medical School, Charlestown, Massachusetts 02129[4]; Division of Comparative Pathology, New England Regional Primate Research Center, Harvard Medical School, Southborough, Massachusetts 01772[5]; Transplantation Biology Research Center, Massachusetts General Hospital, Harvard Medical School, Charlestown, Massachusetts 02129[6]; Department of Medical Oncology, Dana-Farber Cancer Institute, Harvard Medical School, Boston, Massachusetts 02115[7]; Institucio Catalana de Recerca i Estudis Avancats, Barcelona, Spain[8]; and Irsicaixa Foundation, Badalona, Spain[9]

Received 17 October 2008/Accepted 22 April 2009

The generation of humanized BLT mice by the cotransplantation of human fetal thymus and liver tissues and CD34$^+$ fetal liver cells into nonobese diabetic/severe combined immunodeficiency mice allows for the long-term reconstitution of a functional human immune system, with human T cells, B cells, dendritic cells, and monocytes/macrophages repopulating mouse tissues. Here, we show that humanized BLT mice sustained high-level disseminated human immunodeficiency virus (HIV) infection, resulting in CD4$^+$ T-cell depletion and generalized immune activation. Following infection, HIV-specific humoral responses were present in all mice by 3 months, and HIV-specific CD4$^+$ and CD8$^+$ T-cell responses were detected in the majority of mice tested after 9 weeks of infection. Despite robust HIV-specific responses, however, viral loads remained elevated in infected BLT mice, raising the possibility that these responses are dysfunctional. The increased T-cell expression of the negative costimulator PD-1 recently has been postulated to contribute to T-cell dysfunction in chronic HIV infection. As seen in human infection, both CD4$^+$ and CD8$^+$ T cells demonstrated increased PD-1 expression in HIV-infected BLT mice, and PD-1 levels in these cells correlated positively with viral load and inversely with CD4$^+$ cell levels. The ability of humanized BLT mice to generate both cellular and humoral immune responses to HIV will allow the further investigation of human HIV-specific immune responses in vivo and suggests that these mice are able to provide a platform to assess candidate HIV vaccines and other immunotherapeutic strategies.

An ideal animal model of human immunodeficiency virus (HIV) infection remains elusive. Nonhuman primates that are susceptible to HIV infection typically do not develop immunodeficiency (63), and although the simian immunodeficiency virus (SIV) infection of rhesus macaques has provided many critically important insights into retroviral pathogenesis (30), biological and financial considerations have created some limitations to the wide dissemination of this model. The great need for an improved animal model of HIV itself recently has been underscored by the disappointing results of human trials of MRKAd5, an adenovirus-based HIV type 1 (HIV-1) vaccine. This vaccine was not effective and actually may have increased some subjects' risk of acquiring HIV (53). In the wake of these disappointing results, there has been increased interest in humanized mouse models of HIV infection (54). The ability of humanized mouse models to test candidate vaccines or other immunomodulatory strategies will depend critically on the ability of these mice to generate robust anti-HIV human immune responses.

Mice have provided important model systems for the study of many human diseases, but they are unable to support productive HIV infection, even when made to express human coreceptors for the virus (7, 37, 52). A more successful strategy to humanize mice has been to engraft human immune cells and/or tissues into immunodeficient severe combined immunodeficiency (SCID) or nonobese diabetic (NOD)/SCID mice that are unable to reject xenogeneic grafts (39, 42, 57). Early versions of humanized mice supported productive HIV infec-

* Corresponding author. Mailing address: Center for Immunology and Inflammatory Diseases, Division of Rheumatology, Allergy and Immunology, Massachusetts General Hospital, Building 149-8301, 149 13th St., Charlestown, MA 02129. Phone: (617) 724-7368. Fax: (617) 726-5651. E-mail for A. M. Tager: amtager@partners.org. E-mail for A. D. Luster: aluster@mgh.harvard.edu.
† These authors contributed equally.
▽ Published ahead of print on 6 May 2009.

tion and allowed investigators to begin to address important questions in HIV biology in vivo (23, 40, 43–45). More recently, human cord blood or fetal liver $CD34^+$ cells have been used to reconstitute $Rag2^{-/-}$ interleukin-2 receptor γ chain-deficient ($\gamma_c{}^{-/-}$) and NOD/SCID/$\gamma_c{}^{-/-}$ mice, resulting in higher levels of sustained human immune cell engraftment (27, 29, 61). These mice have allowed for stable, disseminated HIV infection (2, 4, 24, 65, 67), including mucosal transmission via vaginal and rectal routes (3). These mice recently have been used to demonstrate an important role for Treg cells in acute HIV infection (29) and to demonstrate that the T-cell-specific delivery of antiviral small interfering RNA is able to suppress HIV replication in vivo (31). These mice also have demonstrated some evidence of adaptive human immune responses, including the generation of HIV-specific antibody responses in some infected mice (2, 65), and some evidence of humoral and cell-mediated responses to non-HIV antigens or pathogens (24, 61). Most impressively, $Rag2^{-/-}$ $\gamma_c{}^{-/-}$ mice reconstituted with human fetal liver-derived $CD34^+$ cells have generated humoral responses to dengue virus infection that demonstrated both class switching and neutralizing capacity (32). In spite of these advances, however, these models have not yet been reported to generate de novo HIV-specific cell-mediated immune responses, which are considered to be a crucial arm of host defense against HIV infection in humans.

In contrast to humanized mouse models in which only human hematopoietic cells are transferred into immunodeficient mice, the surgical implantation of human fetal thymic and liver tissue has been performed in addition to the transfer of human hematopoietic stem cells (HSC) to generate mice in which human T cells are educated by autologous human thymic tissue rather than by the xenogeneic mouse thymus. Melkus and colleagues refer to mice they have reconstituted in this way as NOD/SCID-hu BLT (for bone marrow, liver, and thymus), or simply BLT, mice (41). We previously referred to mice that we have humanized in a similar way as NOD/SCID mice cotransplanted with human fetal thymic and liver tissues (Thy/Liv) and $CD34^+$ fetal liver cells (FLC) (33, 60) but now adopt the designation BLT mice as well. BLT mice demonstrate the robust repopulation of mouse lymphoid tissues with functional human T lymphocytes (33, 41, 60) and can support the rectal and vaginal transmission of HIV (13, 59). Further, BLT mice demonstrate antigen-specific human immune responses against non-HIV antigens and/or pathogens (41, 60). The ability of these mice to generate human immune responses against HIV, however, has not yet been reported. In this study, we investigated whether the provision of autologous human thymic tissue in BLT mice generated by the cotransplantion of human fetal Thy/Liv tissues and $CD34^+$ FLC would allow for the maturation of human T cells in humanized mice capable of providing improved cellular responses to HIV as well as providing adequate help for improved humoral responses. To describe the cells contributing to human immune responses in BLT mice, we also characterized the phenotypes of multiple subsets of T cells, B cells, dendritic cells (DCs), and monocytes/macrophages present in uninfected humanized mice. The generation of robust HIV-directed human cellular and humoral immune responses in these mice would further demonstrate the ability of humanized mice to provide a much needed platform for the evaluation of HIV vaccines and other novel immunomodulatory strategies.

MATERIALS AND METHODS

Mice. We housed NOD/SCID mice (NCI-Frederick) and NOD/SCID/$\gamma_c{}^{-/-}$ mice (kindly provided by Leonard D. Schultz, Jackson Laboratories) in a specific-pathogen-free animal facility at Massachusetts General Hospital. All mice were maintained in microisolator cages, fed autoclaved food and water, and treated according to Institutional Animal Care and Research Committee-approved protocols.

Transplantation of human tissue. BLT mice were generated as previously described (33, 34, 41, 60). Briefly, NOD/SCID mice or NOD/SCID/$\gamma_c{}^{-/-}$ mice at 6 to 8 weeks of age were conditioned with sublethal (2 Gy) whole-body irradiation. They were anesthetized the same day, and ~1-mm^3 fragments of human fetal thymus and liver (17 to 19 weeks of gestational age) (Advanced Bioscience Resources) were implanted under the recipient kidney capsules bilaterally. Remaining fetal liver tissue was used to isolate $CD34^+$ cells with anti-CD34 microbeads (Miltenyi Biotec), which then were injected intravenously (1.0×10^5 to 5.0×10^5 cells/mouse) within 6 h.

Human immune reconstitution and immunophenotyping. Human immune cell engraftment was monitored by flow cytometry by determining the percentages of human $CD45^+$ cells that were within the lymphocyte gates of forward versus side scatter plots of peripheral blood. Prior to flow cytometry, blood samples were stained with directly conjugated anti-mouse CD45-phycoerythrin-Cy7 (CD45-PE-Cy7) or CD45-allophycocyanin (CD45-APC), as well as anti-human CD45-fluorescein isothiocyanate (CD45-FITC), CD3-Pacific Blue or CD3-PE, CD4-APC-Cy5 or CD4-APC-Alexa 700, CD8-APC-Cy7, CD14-PE, CD19-PE/Cy5, and CD20-APC (BD Pharmingen). The immunophenotyping of cells in BLT mouse spleens, lymph nodes (LNs), thymic grafts, and bone marrow was performed after the passage of these tissues through 70-μm filters. Human spleen and bone marrow tissues for comparison to BLT mouse tissues were obtained through the kind courtesy of Nancy L. Harris and David Scadden (Massachusetts General Hospital, Boston), respectively. Protocols involving the use of human tissues were approved by the Massachusetts General Hospital Human Research Committee. Mononuclear cells were isolated from spleen cell suspensions by centrifugation through a density gradient on Histopaque-1077 (Sigma-Aldrich), except for B-cell populations. Splenocytes and bone marrow cells for B-cell phenotyping experiments were isolated and processed as previously described (11). Other antibodies used for immunophenotyping included directly conjugated anti-human CD3-APC/Cy7, CD11c-PE, CD14-Pacific Blue, CD27-APC-Cy7, CD34-APC or CD34-PE, CD45-APC, CD45R-FITC (which cross-reacts with mouse and human), CD45RA-PE-Cy5, CD69-PE, CD123-APC, C-C chemokine receptor 7-PE (CCR7-PE), CXCR4-APC, CCR5-PE-Cy7, HLA-DR-FITC, HLA-DR-peridinin chlorophyll protein-Cy5.5 (all from BD Pharmingen), CD16-PE-Cy7 (Biolegend), and programmed death 1-PE (PD-1-PE) (clone EH12; G. Freeman) (14). Antibodies for B-cell immunophenotyping were directly conjugated anti-human CD19-APC-H7, CD10-PE, CD20-PE-Cy7, CD27-APC, and CD38-PE (BD Pharmingen) and immunoglobulin M-FITC (IgM-FITC), IgD-FITC, IgD-PE, and IgG-FITC (Dako). Intracellular staining was performed on cells that were fixed and permeabilized with Fix & Perm (Caltag) with directly conjugated anti-human Ki-67-FITC (Dako), perforin-FITC, or IFN-γ-FITC (BD Pharmingen). Data were acquired on an LSRII (Becton Dickinson) and analyzed with FlowJo software (Tree Star), except for B-cell immunophenotyping data, which was acquired on a FACSCanto II (Becton Dickinson) and analyzed using previously described gating strategies (8–10).

HIV infection. When peripheral blood percentages of human T cells reached a plateau at their maximal values, which generally occurred 13 to 14 weeks posttransplantation, BLT mice were inoculated intraperitoneally with the R5-tropic HIV strain JRCSF (HIV_{JRCSF}) (2,000 or 10,000 50% tissue culture infectious doses [$TCID_{50}$]) or HIV_{ADA} (50,000 or 75,000 $TCID_{50}$). Following inoculation, mice were bled weekly to obtain plasma for HIV viral load measurements using the Cobas Amplicor reverse transcription-PCR (RT-PCR) assay (Roche Diagnostics) and leukocytes for immunophenotyping.

Immunohistochemistry and in situ hybridization. Immunoperoxidase staining was performed on 5-μm formalin-fixed paraffin-embedded step sections from infected and uninfected BLT mice using standard avidin-biotin peroxidase complex techniques (Dako). Sections were incubated with anti-human CD3 (rabbit polyclonal; Dako), CD4 (1F6 IgG1; Vector Laboratories), CD8 (1A5 IgG1; Vector Laboratories), CD20 (L26 IgG2a; Dako), or CD68 (KP1 IgG1; Dako) antibody. Sections stained with anti-CD3 antibody were incubated with biotinylated goat anti-rabbit secondary antibody (Vector), and sections stained with anti-CD4, CD8, CD20, or CD68 antibody were incubated with biotinylated isotype-matched horse anti-mouse IgG secondary antibodies (Vector). Tissue sections were washed, developed with DAB chromogen (Dako), and counterstained with Mayer's hematoxylin. Isotype-matched irrelevant controls were included for all tissues. Anti-human anti-

bodies also were tested for their specificity for human and mouse antigens on tissues from unreconstituted mice. Immunohistochemical staining of HIV Gag p24 capsid protein in paraffin sections of spleens from infected BLT mice was performed with anti-p24 antibody Kal-1 (Dako) as described previously (46). The identification of HIV by the in situ hybridization of antisense probes spanning the entire HIV genome (Lofstrand Labs), with the concurrent identification of $CD3^+$ T cells or Ham-56^+ macrophages by immunohistochemistry, also was performed as previously described (47).

Detection of humoral and cellular immune responses. HIV-specific IgG, IgM, and IgA human antibodies were detected in plasma samples from HIV-infected BLT mice using Genetic Systems HIV-1 Western Blot kits (Bio-Rad) according to the manufacturer's instructions. Antibodies were detected in a final dilution of mouse plasma of 1:101, the same dilution as that recommended by the manufacturer for the detection of HIV-specific antibodies in human clinical samples. HIV-specific human T cells were identified in mononuclear cells pooled from the blood, spleen, and LNs of individual mice. Enzyme-linked immunospot (ELISPOT) assays were performed as previously described, using 100,000 cells per well (17). Peptide pools consisting of overlapping 15- to 20-mers spanning all expressed HIV proteins in the consensus clade B sequence, or the autologous HIV_{ADA} sequences of *gag* and *nef*, were used in a previously described peptide matrix approach (20). To identify T-cell responses specific to single HIV peptides and determine whether these responses were mediated by $CD4^+$ or $CD8^+$ cells, additional ELISPOT assays or intracellular cytokine staining assays for gamma interferon (IFN-γ) were performed the following day, as previously described (20).

Statistical analysis. Student's *t* test (paired and unpaired, as indicated) and Pearson's correlation coefficient (*r*) were determined using Excel software (Microsoft) to assess statistical significance. All *t* tests were two tailed, and $P < 0.05$ was considered significant.

RESULTS

Human immune reconstitution in BLT mice. Previous studies have demonstrated high levels of human immune cell engraftment in BLT mice following the transplantation of human fetal thymic and liver tissue and $CD34^+$ FLC (33, 34, 41, 60). We found that BLT mice demonstrate the high-level engraftment of multiple human immune cell lineages, including progenitor cells in their bone marrow and thymic grafts, and differentiated T cells, B cells, DCs, and monocytes/macrophages in their peripheral tissues.

Progenitor cell reconstitution. Both the bone marrow and thymic grafts of BLT mice maintained robust populations of human progenitor cells over time. At 22 weeks posttransplantation, the proportion of human $CD45^{dim}$, $CD34^+$ HSCs among lymphoid-gated cells in the bone marrow was 7.6% ± 1.2% (means ± standard errors; $n = 3$) (Fig. 1A, image i). HSCs also are characterized as having low side scatter in addition to being $CD45^{dim}$ and $CD34^+$ (21, 36), and the proportion of human HSCs in BLT bone marrow was confirmed by identifying $CD34^+$ cells among $CD45^{dim}$ cells with low side scatter. In the representative mouse presented in Fig. 1A, image ii, 14.0% of lymphoid-gated cells were $CD45^{dim}$ with low side scatter, and 48.4% of these $CD45^{dim}$, low-side-scatter cells were $CD34^+$, thus identifying 6.8% of lymphoid-gated cells as HSCs (48.4% of 14.0% = 6.8%). Since subsets of naïve B cells can share these phenotypic markers with HSCs (35), we used the B-cell marker CD45R (6, 49) to further distinguish $CD45R^-$ stem cells from $CD45R^+$ B cells in these populations. Almost all of the $CD45^{dim}$, low-side-scatter, $CD34^+$ cells were negative for CD45R (Fig. 1A, image ii), confirming that these cells were HSCs. Cells with a similar HSC phenotype also were found in the spleens of BLT mice, though in smaller numbers (2.1% ± 0.6%; $n = 3$) (Fig. 1B) than in the bone marrow.

During the reconstitution of BLT mice with human immune cells, their transplanted thymic grafts grew in size quite substantially, as demonstrated for a representative mouse in Fig. 1C. Analyses of the human thymic grafts demonstrated high percentages of human $CD4^+$ $CD8^+$ double-positive thymocytes (Fig. 1D), similarly to human thymic tissue (19).

T-cell reconstitution. We next identified human T and B cells in BLT mice, also using polychromatic flow cytometry, with the gating scheme shown in Fig. 2A for a representative sample of peripheral blood cells from a mouse 22 weeks posttransplantation. Consistently with prior reports, the BLT mice generated for the studies we report here also demonstrated high proportions of human $CD45^+$ cells among the lymphocyte populations in the blood, spleen, and lymph nodes that continued to increase up to 22 weeks posttransplantation ($n = 5$ to 12 mice per time point) (Fig. 2B). NOD/SCID/$\gamma_c^{-/-}$ mice, which lack NK cell activity, have been reported to support improved human immune engraftment compared to that of NOD/SCID mice (26, 56). In our reconstitutions, however, human lymphocyte engraftment was similar in mice of both of these immunodeficient backgrounds (data not shown). At ≥14 weeks posttransplant, the majority of the human $CD45^+$ lymphocytes in the blood and lymph nodes were T cells (Fig. 2C). We also determined the differentiation state of T cells in the humanized BLT mice while they were housed in a specific-pathogen-free environment. At 18 weeks after transplantation, most of the human $CD4^+$ and $CD8^+$ T cells in the spleens had a naïve phenotype ($CD45RA^+$, $CD27^+$), with almost all expressing CCR7 (Fig. 2D). With respect to their expression of the HIV coreceptors CXCR4 and CCR5, both $CD4^+$ and $CD8^+$ T cells had high levels of CXCR4 and low levels of CCR5 expression, consistently with their predominantly naïve phenotype.

B-cell reconstitution. We compared B-cell development in BLT mice to that in adult humans in both the bone marrow and the spleen (Fig. 3). The absence of mature recirculating human B cells in the bone marrow previously has been reported in NOD/SCID mice humanized with cord blood $CD34^+$ cells (50). In contrast, the various stages of B-cell development seen in the bone marrow of BLT mice included fully mature B cells and plasmablasts, although B cells at earlier developmental stages were overrepresented and terminally differentiated, long-lived bone marrow plasma cells were not detected. In the BLT mouse bone marrow, more than 50% of the cells in the lymphoid gate were human $CD19^+$ B cells (64.3% ± 2.6%; $n = 3$) (Fig. 3A, image i, left), which is in agreement with prior reports of BLT mice (41) and other humanized mouse models (26, 50, 56). In contrast, the proportion of $CD19^+$ cells in the lymphoid gate of bone marrow samples obtained from adult humans was approximately 11.3% ± 0.2% ($n = 3$) (Fig. 3A, image ii, left). Most of the $CD19^+$ B cells in BLT mouse bone marrow also were $CD10^+$ (data not shown), suggesting that they were immature (35); the numbers of mature, human $CD19^+$, $CD20^+$ B cells, however, were comparable in BLT mouse (7.5% ± 0.3%; $n = 3$) and human (8.0% ± 0.2%; $n = 3$) bone marrow (Fig. 3A, images i and ii, right). Long-lived mature follicular B cells are part of the recirculating B-cell pool in the bone marrow (10) and can be divided into two distinct populations based on surface IgM and IgD levels: follicular type I (FO-I) cells are IgM^{lo} and IgD^{hi}, and follicular type II (FO-II) cells are IgM^{hi} and IgD^{hi} (8). The IgM and IgD

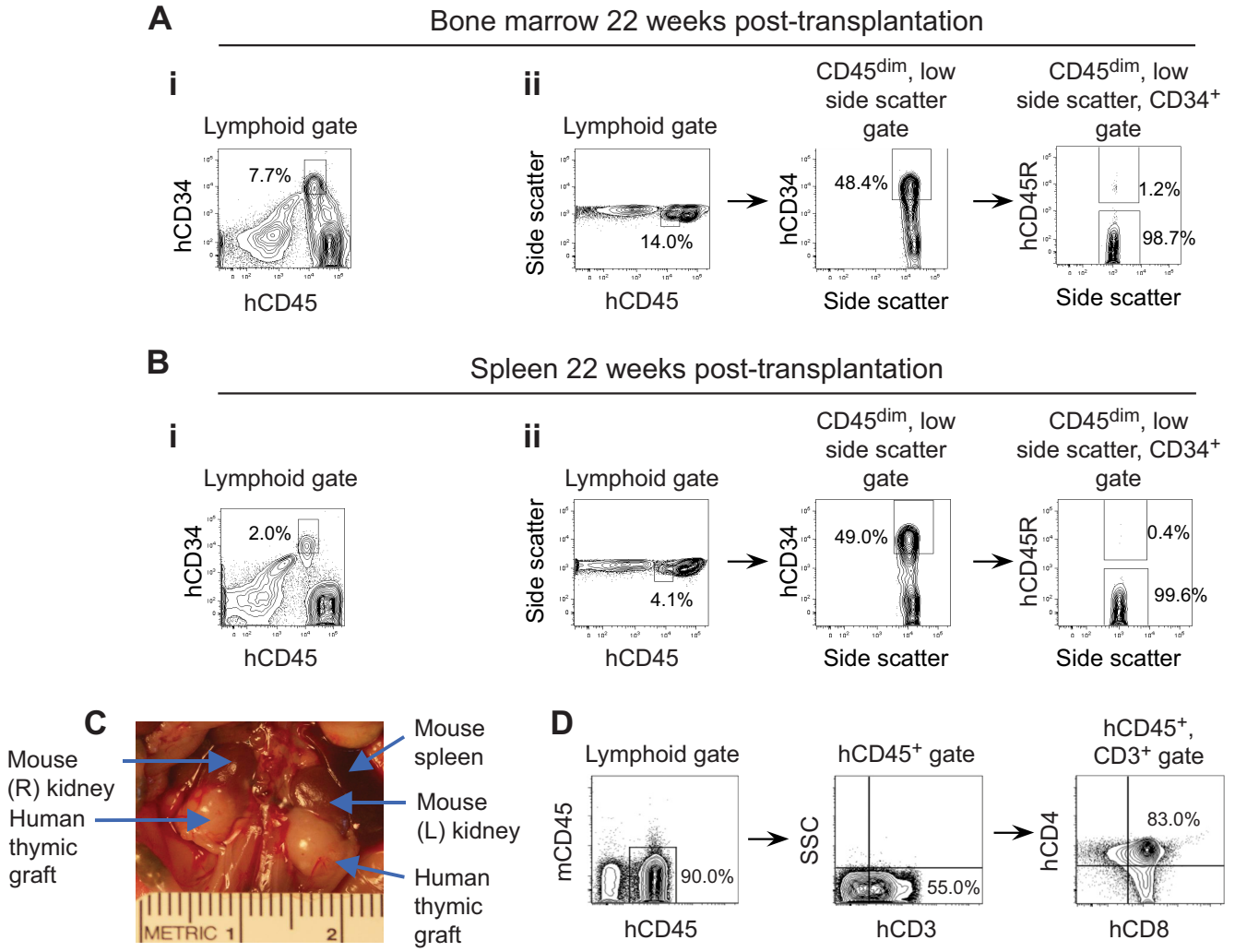

FIG. 1. Human progenitor cell reconstitution of BLT mice. (A) HSC engraftment 22 weeks posttransplantation in the bone marrow of BLT mice. HSC are identified in image i as $CD45^{dim}$, $CD34^+$ cells among lymphoid-gated cells and in image ii as $CD45^{dim,}$ low-side-scatter, $CD34^+$ cells. Numbers in the panels represent percentages of cells contained in the indicated gates. Data presented are representative of $n = 3$ mice. (B) HSC engraftment 22 weeks posttransplantation in the spleens of BLT mice. HSC are identified in images i and ii as described for panel A. Data presented are representative of $n = 3$ mice. (C) Gross appearance of bilateral thymic grafts in a representative BLT mouse following reconstitution with human immune cells, demonstrating substantial growth in size from the ~1-mm^3 fragments of human fetal tissues transplanted. (D) CD4 and CD8 expression of human thymocytes in the thymic graft of a representative BLT mouse 14 weeks after transplantation.

expression profile of human $CD19^+$, $CD20^+$ B cells in the bone marrow of BLT mice demonstrated the presence of both FO-I and FO-II cells, although fewer FO-I cells were present (6.7% ± 1.0% and 6.2% ± 0.9% of $CD19^+$, $CD20^+$ cells at 20 and 22 weeks, respectively; $n = 3$ at each time point) (Fig. 3B, image i) than in adult human bone marrow (24.2% ± 1.9%; $n = 3$) (Fig. 3B, image ii). The numbers of FO-II cells present in the bone marrow of BLT mice were greater at 22 weeks posttransplantation (13.3% ± 1.3%) than at 20 (7.6% ± 0.6%) or 16 weeks (data not shown), suggesting that B-cell maturation increases in BLT mice with a longer duration of reconstitution. We next examined the numbers of IgM^+, $CD27^+$ B cells (IgM memory cells/marginal zone B cells) and $CD27^+$, IgM^+, IgD^+, IgG^+, $CD38^{hi}$ cells (plasmablasts) in the bone marrow of both BLT mice and humans (Fig. 3C, images i and ii). The proportion of marginal-zone B cells was comparable between BLT mice and humans (3.7% ± 0.9% and 4.2% ± 0.1% of $CD27^+$ cells, respectively) (Fig. 3C, image i and ii, left). Differentiation into plasmablasts did occur in the bone marrow of BLT mice but to a lesser extent than in humans: plasmablasts represented 0.6% ± 0.6% of $CD27^+$, IgM^+, IgD^+, IgG^+ bone marrow cells in BLT mice and 7.1% ± 0.4% in humans ($n = 3$ in each case) (Fig. 3C, images i and ii, right).

In contrast to the bone marrow, there were similar proportions of both human $CD19^+$ B cells (mouse, 48.1% ± 2.7%; human, 46.9% ± 2.4%) and more mature $CD19^+$, $CD20^+$ cells (mouse, 29.9% ± 2.3%; human [$CD20^{hi}$ + $CD20^{int}$], 40.6% ± 4.1%; $n = 3$) (Fig. 3D, images i and ii) among the lymphoid-gated cells in the spleens of BLT mice and in adult human spleens obtained following splenectomies, although a higher proportion of $CD19^+$ cells in the BLT spleens were $CD10^+$ immature B cells (data not shown). The IgM and IgD expres-

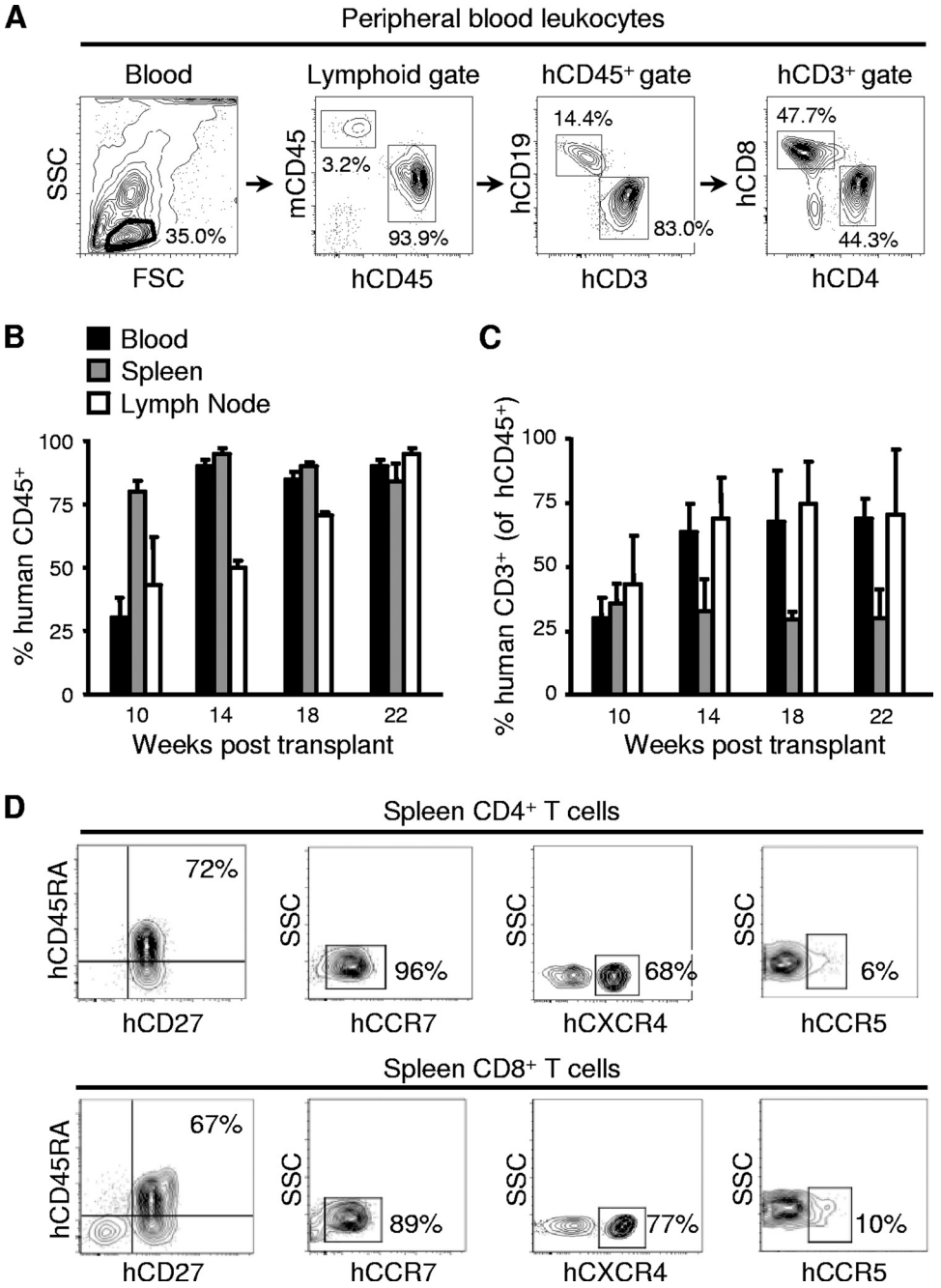

FIG. 2. Human T-cell reconstitution of BLT mice. (A) The multiparameter flow cytometry gating scheme for the identification of human lymphocyte populations in BLT mice is shown for a representative sample of peripheral blood from a mouse 22 weeks posttransplantation. Numbers in the panels represent percentages of cells contained in the indicated gates. SSC, side scatter; FSC, forward scatter. (B, C) BLT mice were sacrificed at the indicated times posttransplantation, and human cells were identified in blood, spleen, and LN by flow cytometry following staining with human $CD45^+$ antibody. Data in panel B are presented as the percentages of human $CD45^+$ cells among blood, spleen, and LN lymphocyte populations; data in panel C are presented as the percentages of human $CD3^+$ T cells among human $CD45^+$ leukocytes. Data represent mean values ± standard errors for $n = 5$ to 12 mice per group. (D) Analyses of naïve versus memory phenotypes and chemokine receptor expression of $CD4^+$ and $CD8^+$ T cells from the spleen of a representative humanized BLT mouse 18 weeks after transplantation.

sion profile of human $CD19^+$, $CD20^+$, $CD27^-$ B cells in the spleens of BLT mice also demonstrated the presence of both FO-I and FO-II mature human follicular B cells (FO-I, 21.0% ± 0.9% and 18.6% ± 1.8% of $CD19^+$, $CD20^+$, $CD27^-$ cells at 20 and 22 weeks, respectively, and FO-II, 44.1% ± 0.9% and 39.1% ± 2.6% at 20 and 22 weeks, respectively; $n = 3$ at both time points) (Fig. 3E, image i). IgM^+, $CD27^+$ memory/marginal zone B cells also were present in the spleen (90.2% ± 1.7% and 89.4% ± 1.8% of $CD27^+$ cells at 20 and 22 weeks, respectively; $n = 3$) (Fig. 3F). Taken together, these

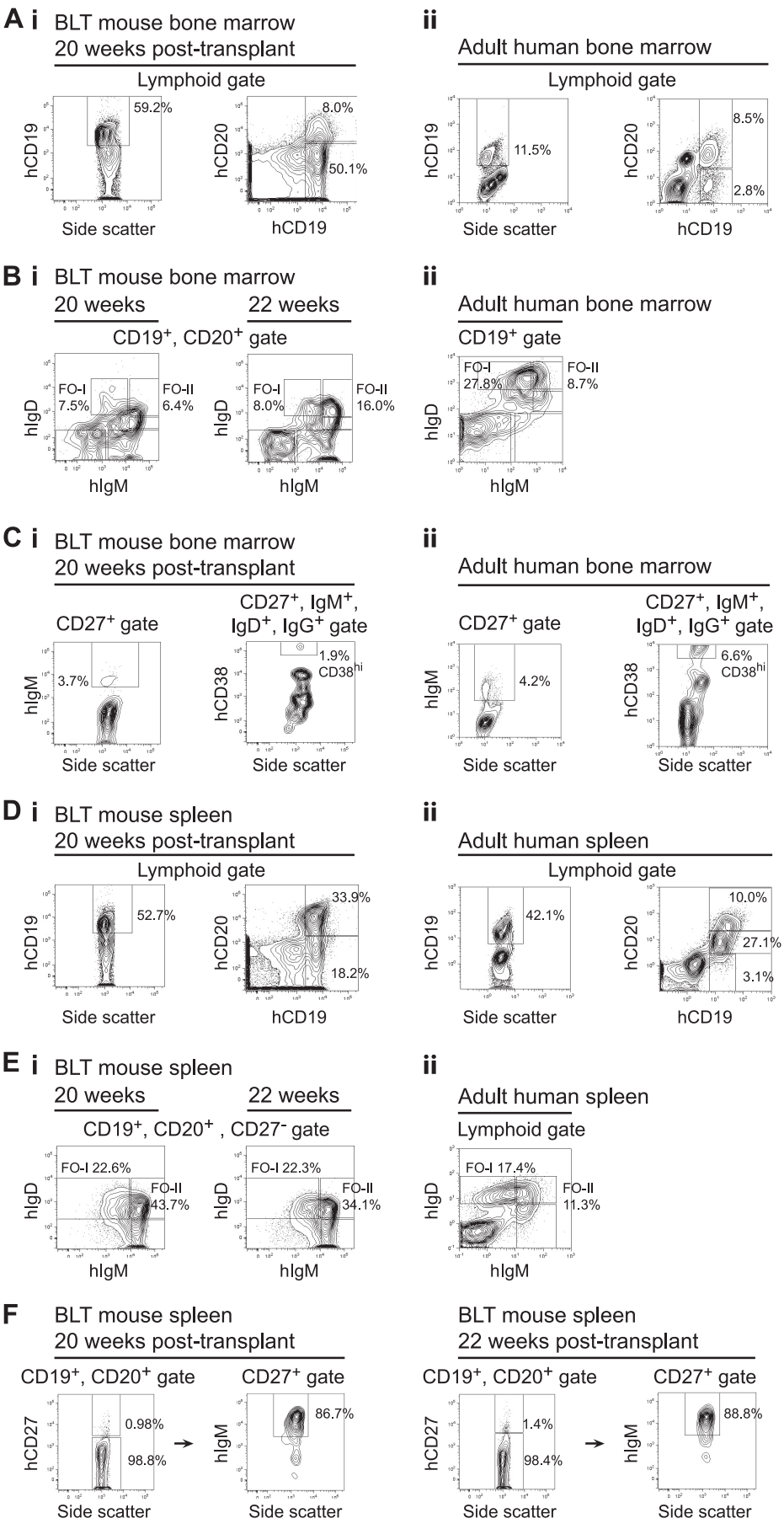
A i
BLT mouse bone marrow
20 weeks post-transplant
Lymphoid gate
59.2%
hCD19
Side scatter
8.0%
50.1%
hCD20
hCD19
ii
Adult human bone marrow
Lymphoid gate
11.5%
hCD19
Side scatter
8.5%
2.8%
hCD20
hCD19
B i
BLT mouse bone marrow
20 weeks
22 weeks
CD19+, CD20+ gate
FO-I 7.5%
FO-II 6.4%
hIgD
hIgM
FO-I 8.0%
FO-II 16.0%
hIgD
hIgM
ii
Adult human bone marrow
CD19+ gate
FO-I 27.8%
FO-II 8.7%
hIgD
hIgM
C i
BLT mouse bone marrow
20 weeks post-transplant
CD27+ gate
3.7%
hIgM
Side scatter
CD27+, IgM+, IgD+, IgG+ gate
1.9%
CD38hi
hCD38
Side scatter
ii
Adult human bone marrow
CD27+ gate
4.2%
hIgM
Side scatter
CD27+, IgM+, IgD+, IgG+ gate
6.6%
CD38hi
hCD38
Side scatter
D i
BLT mouse spleen
20 weeks post-transplant
Lymphoid gate
52.7%
hCD19
Side scatter
33.9%
18.2%
hCD20
hCD19
ii
Adult human spleen
Lymphoid gate
42.1%
hCD19
Side scatter
10.0%
27.1%
3.1%
hCD20
hCD19
E i
BLT mouse spleen
20 weeks
22 weeks
CD19+, CD20+ , CD27- gate
FO-I 22.6%
FO-II 43.7%
hIgD
hIgM
FO-I 22.3%
FO-II 34.1%
hIgD
hIgM
ii
Adult human spleen
Lymphoid gate
FO-I 17.4%
FO-II 11.3%
hIgD
hIgM
F
BLT mouse spleen
20 weeks post-transplant
CD19+, CD20+ gate
0.98%
98.8%
hCD27
Side scatter
CD27+ gate
86.7%
hIgM
Side scatter
BLT mouse spleen
22 weeks post-transplant
CD19+, CD20+ gate
1.4%
98.4%
hCD27
Side scatter
CD27+ gate
88.8%
hIgM
Side scatter

analyses suggest that the maturation and differentiation of human B cells in the bone marrow and spleens of the BLT mice are comparable to those occurring in these organs in humans, although there is a greater frequency of immature B cells in humanized mice.

DC reconstitution. As demonstrated in Fig. 4A, both $CD11c^+$ myeloid DCs (mDCs) and $CD123^+$ plasmacytoid DCs (pDCs) could be identified among human $CD45^+$, lineage-negative ($CD16^-$, $CD3^-$, $CD19^-$), $HLA\text{-}DR^+$ cells in the BLT mice in analyses similar to those described in reference 22. At 20 weeks posttransplantation, 1.9% ± 0.6% of human $CD45^+$ cells in the blood of BLT mice and 2.2% ± 0.3% of human $CD45^+$ cells in the spleens were mDCs, whereas pDCs represented 0.2% ± 0.1% of human $CD45^+$ cells in the blood and 0.3% ± 0.1% of human $CD45^+$ cells in the spleens ($n = 3$ for both blood and spleens) (Fig. 4B). Similarly, greater numbers of mDCs than pDCs have been noted in the blood of humans (22).

Monocyte/macrophage reconstitution. The expression of the lipopolysaccharide receptor (CD14) and of Fcγ receptor III (CD16) were used to identify human monocytes/macrophages in the lungs of BLT mice (Fig. 4C), which were chosen as a peripheral tissue that contains large populations of these cells. Classical monocytes are $CD14^{high}$, $CD16^-$, whereas $CD14^{dim}$, $CD16^+$ monocytes are thought to be more mature macrophage-like cells and are regarded as proinflammatory (25). At 20 weeks posttransplantation, 25.4% ± 2.1% of human $CD45^+$ cells in the lungs of BLT mice were $CD14^{high}$, $CD16^-$ monocytes, and 12.9% ± 0.8% were $CD14^{dim}$, $CD16^+$ monocytes ($n = 3$) (Fig. 4D). The $CD14^{high}$, $CD16^-$ classical monocyte subset, which represents the majority of monocytes in human peripheral blood (25), thus was the most common subset of human monocytes/macrophages in the lungs of BLT mice.

The high-level engraftment of human $CD3^+$ T cells, $CD4^+$ T cells, $CD8^+$ T cells, CD 20^+ B cells, and $CD68^+$ macrophages in the LN and spleens of BLT mice was confirmed by the immunohistochemical staining of these tissues (Fig. 5). Immunostaining also demonstrated the engraftment of these human immune cells in the gastrointestinal tract of BLT mice (Fig. 5).

Sustained, high-level infection of BLT mice with CCR5-tropic HIV. Humanized BLT mice were infected with escalating doses of HIV to determine an optimal infecting dose in our model. We used CCR5-tropic (R5-tropic) viruses, since these strains are most relevant in early HIV infection. Mice were bled at weekly intervals postinoculation (p.i.), and plasma viral loads were determined by RT-PCR. At an infecting dose of 2,000 $TCID_{50}$, 30% of mice injected with HIV_{JRCSF} ($n = 10$) became productively infected (defined as having a detectable viral load) as shown in Fig. 6A. At a dose of 75,000 $TCID_{50}$, 100% of humanized mice injected with HIV_{ADA} ($n = 20$) became productively infected (Fig. 6A). Inoculation with 2,000 $TCID_{50}$ of HIV_{JRCSF} resulted in a mean peak plasma viral copy number of 1.1×10^4 at 6 weeks p.i. among mice that were productively infected ($n = 3$), as shown in Fig. 6B. The injec-

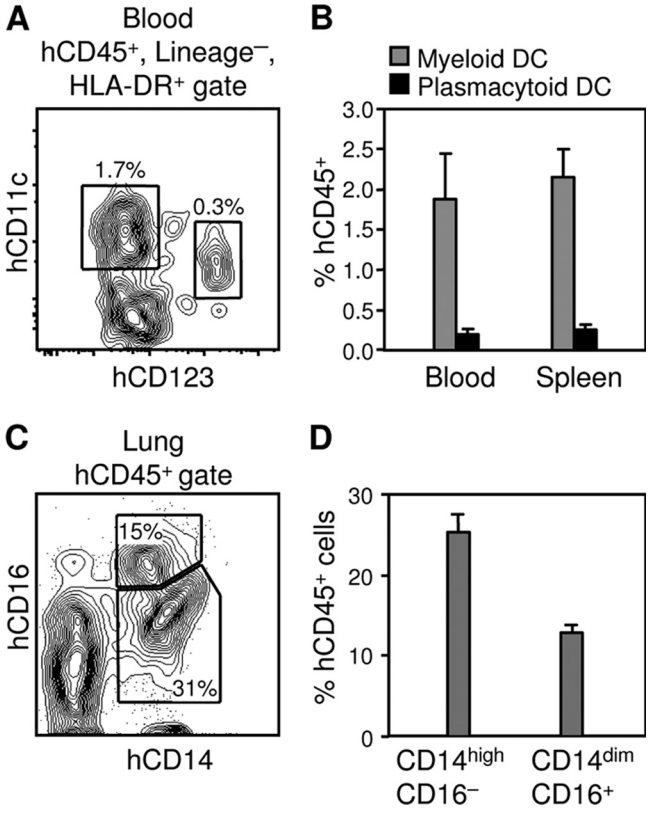

FIG. 4. DC and monocyte/macrophage reconstitution of BLT mice. (A) Identification of human mDCs and pDCs in the peripheral blood of a BLT mouse 20 weeks posttransplantation. mDCs are identified as $CD11c^+$ cells, and pDCs are identified as $CD123^+$ cells among human $CD45^+$, lineage-negative ($CD16^-$, $CD3^-$, $CD19^-$), $HLA\text{-}DR^+$ cells. Numbers in the panel represent the percentages of cells contained in the indicated gates. (B) mDC and pDC engraftment in the blood and spleens of BLT mice 20 weeks posttransplantation. Data represent means ± standard errors for $n = 3$ mice. (C) Identification of human monocytes/macrophages in the lungs of a BLT mouse 20 weeks posttransplantation. Numbers in the panel represent the percentages of cells contained in the indicated gates. (D) Engraftment of $CD14^{high}$, $CD16^-$ classical monocytes and mature macrophage-like $CD14^{dim}$, $CD16^+$ monocytes in the lungs of BLT mice 20 weeks posttransplantation. Data represent means ± standard errors for $n = 3$ mice.

FIG. 3. Human B-cell reconstitution of BLT mice bone marrow and spleen. Bone marrow cells in panels A, B, and C and splenocytes in panels D, E, and F were analyzed by flow cytometry. Results for BLT mice are presented in image i and are compared to results for cells from adult human tissues in image ii. BLT mouse and adult human tissues were analyzed in independent experiments; all antibodies used were anti-human. Numbers in the panels are the percentages of cells in the indicated gates. Data presented are representative of $n = 3$ BLT mice at each time point (20 and 22 weeks posttransplantation) and $n = 3$ humans. All BLT mouse panels for a give time point represent data from the same mouse. $CD19^+$ and $CD19^+$, $CD20^+$ B cells were identified in panels A and D, follicular-zone B cells were identified in panels B and E, marginal-zone B cells were identified in panels C and F, and plasmablasts were identified in panel C. In image i of panel C, the percentage of marginal-zone B cells demonstrated in the left flow plot (3.7%) corresponds to 63 out of 1,707 total events shown, and the percentage of plasmablasts demonstrated in the right flow plot (1.9%) corresponds to 1 out of 54 total events shown. Gates were drawn as previously published (8–10).

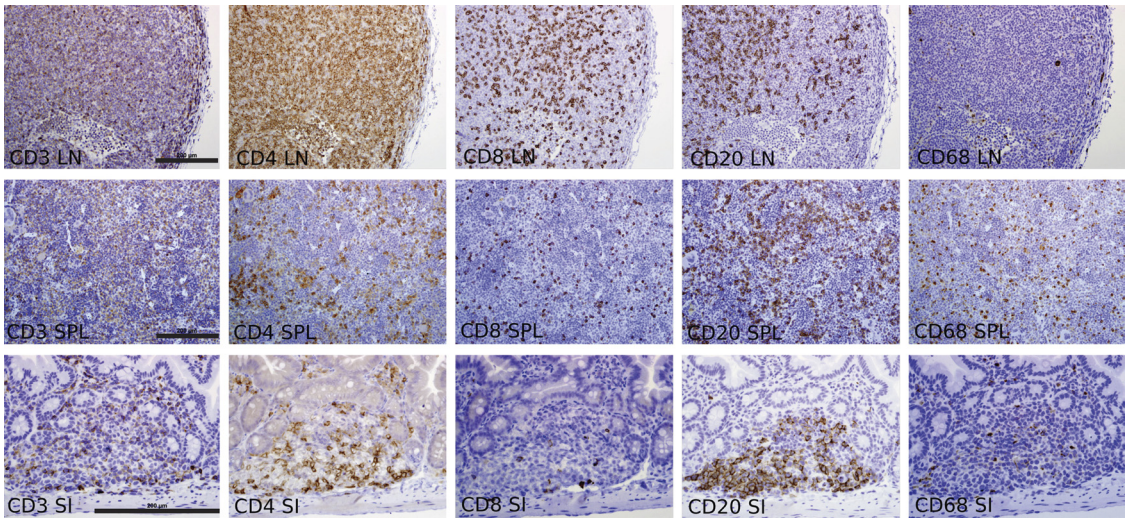

FIG. 5. Histology of human immune cell reconstitution in the LN, spleen, and gastrointestinal tract of BLT mice. Immunohistochemical staining of LN, spleens (SPL), and small intestine (SI) of BLT mice 20 to 22 weeks posttransplantation for the indicated human antigens demonstrated the robust reconstitution of $CD3^+$ T cells, $CD4^+$ T cells, $CD8^+$ T cells, $CD20^+$ B cells, and $CD68^+$ macrophages (all bars = 200 μm; the magnification is the same for each panel from a given tissue).

tion of 50,000 and 75,000 $TCID_{50}$ of HIV_{ADA} resulted in mean peak viral loads of $>2.2 \times 10^5$ and $>1.5 \times 10^6$ at 6 weeks p.i., respectively ($n = 3$ to 7 mice per group at each time point) (Fig. 6B). Mice infected with 75,000 $TCID_{50}$ of HIV_{ADA} maintained high levels of plasma viremia for up to 4 months p.i. All infections subsequently were performed with 75,000 $TCID_{50}$ HIV_{ADA}. To assess the dissemination of HIV to the lymphoid organs of infected BLT mice, we identified HIV-infected cells by in situ hybridization to HIV RNA. Costaining for CD3 (Fig. 6C to F) revealed that infected cells were $CD3^+$ and were distributed primarily in the T-cell-rich periarteriolar lymphoid sheaths of the spleen (Fig. 6C, D) and throughout the heavily

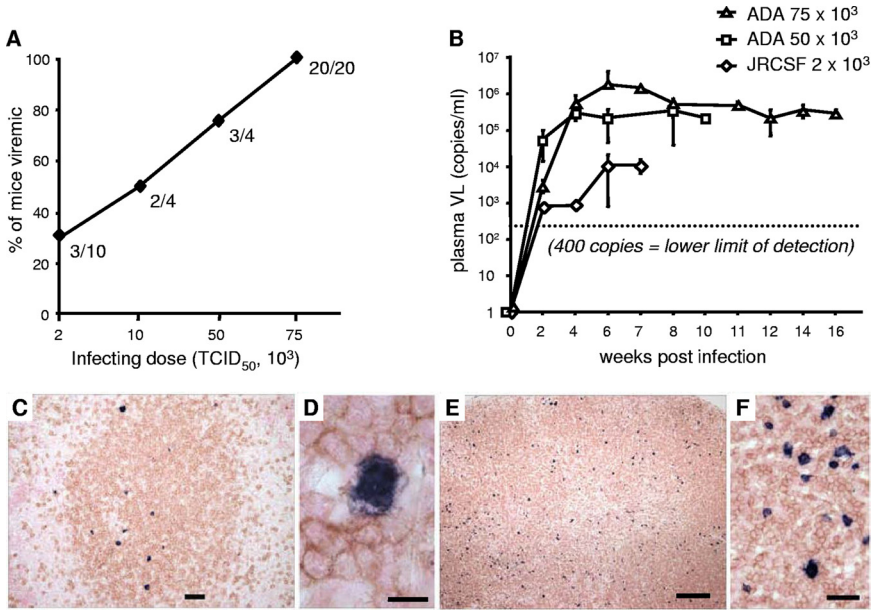

FIG. 6. Sustained, high-level, disseminated HIV infection of BLT mice. (A) Humanized BLT mice were injected intraperitoneally with HIV_{JRCSF} (2000 and 10,000 $TCID_{50}$) or HIV_{ADA} (50,000 and 75,000 $TCID_{50}$) and bled weekly for the following 8 weeks to assess detectable plasma viremia. Data are presented as the percentages of mice inoculated with each infecting dose that developed detectable viral loads (VL). (B) Plasma viral loads were measured every 1 to 2 weeks following inoculation of BLT mice with the indicated HIV isolate and infecting dose. The dotted line indicates the lower limit of detection for the RT-PCR assay (400 copies/ml). Data represent mean values ± standard errors for three to seven mice analyzed at each time point. (C to F) Identification of HIV-infected cells by in situ hybridization for HIV RNA, and the concurrent identification of human T cells by immunohistochemical staining for human CD3, demonstrated HIV-infected human T cells in the periarteriolar lymphoid sheath of the spleen and diffusely distributed in the LN of a representative HIV-infected BLT mouse. Bars: panel C, 100 μm; panel D, 10 μm; panel E, 200 μm; panel F, 20 μm.

T-cell-reconstituted LNs (Fig. 6E, F). In contrast, infected cells in spleens and LNs were negative when costained with the macrophage marker Ham-56 (data not shown). We confirmed the dissemination of HIV to the lymphoid organs of infected BLT mice with the immunohistochemical staining of HIV Gag-p24 antigen (data not shown).

$CD4^+$ T-cell depletion following HIV infection. R5-tropic HIV infection was associated with the depletion of human $CD4^+$ T cells in the blood of BLT mice. Declines in $CD4^+$ T-cell percentages in the circulation began at 6 weeks p.i. and continued through 16 weeks p.i. ($n = 5$ to 18 mice per time point) (Fig. 7A). Total numbers of circulating lymphocytes determined in a subset of HIV-infected mice ($n = 5$), however, remained normal or only slightly decreased (data not shown), suggesting that the numbers of $CD8^+$ T cells and/or B cells increased while the numbers of $CD4^+$ T cells decreased. We also examined the effect of HIV infection on the expression of CCR5 by circulating T cells in the humanized mice. At 3 weeks p.i., we found that CCR5 expression by $CD4^+$ T cells fell more than 10-fold, from 6.8% ± 2.3% in uninfected mice to 0.4% ± 0.2% in infected mice, consistently with the depletion of $CCR5^+$ $CD4^+$ T cells by infection with the R5-tropic virus used, whereas CCR5 expression on $CD8^+$ T lymphocytes remained unchanged (Fig. 7B). Interestingly, at 16 weeks p.i., CCR5 expression was significantly increased in both $CD4^+$ (to 44.8% ± 12.2%) and $CD8^+$ T cells (to 80.3% ± 8.1%). Increased percentages of $CD4^+$ T cells expressing CCR5 also has been noted in primary HIV infection in humans, despite the predominance of R5-tropic HIV strains in these infections (66). The conversion of naive $CCR5^-$ cells to an antigen-experienced $CCR5^+$ phenotype appears to contribute to the increased percentages of $CD4^+$ T cells expressing CCR5 that are observed in primary human infection (66), consistently with the state of generalized immune activation associated with human HIV infection (15). T-cell CCR5 expression data in these experiments were obtained from 3 to 6 mice at each time point.

T-cell activation following HIV infection. HIV infection in humans is associated with widespread immune activation as noted above (15), and this immune activation has been implicated in HIV disease progression (16). The increased T-cell CCR5 expression that we observed in the HIV-infected BLT mice at 16 weeks p.i. suggested that HIV infection causes immune activation in these mice as well, and therefore we investigated further whether circulating T cells are activated by HIV infection in BLT mice. All mice had achieved full reconstitution and had stable T-cell phenotypes prior to infection. We then analyzed the expression of multiple phenotypic markers by the $CD8^+$ and $CD4^+$ T cells in two matched blood samples obtained from the same BLT mice, the first obtained before HIV infection and the second 12 weeks p.i. ($n = 3$ to 5 mice per phenotypic marker analyzed) (Fig. 7C to G). The nuclear antigen Ki-67 is expressed specifically by actively proliferating cells, and its expression by T cells in BLT mice increased significantly following HIV infection: the percentage of $CD8^+$ T cells expressing Ki-67 increased from 15.3% ± 3.2% in uninfected mice to 57.4% ± 5.4% in mice 12 weeks p.i.; the percentage of $CD4^+$ T cells expressing Ki-67 increased from 12.3% ± 3.4% to 48.8% ± 9.1% (Fig. 7C). CD27 typically is downregulated on T cells in the setting of prolonged antigen stimulation, and its expression significantly decreased in BLT mice following infection: the percentage of $CD8^+$ T cells that were $CD27^+$ decreased from 98.6% ± 0.2% in uninfected mice to 84.6% ± 3.8% in mice 12 weeks p.i.; the percentage of $CD4^+$ T cells that were $CD27^+$ decreased from 98.0% ± 0.4% to 78.9% ± 2.9% (Fig. 7D). The expression of the early activation markers CD69 (Fig. 7E) and HLA-DR (Fig. 7F) increased significantly on $CD8^+$ T cells in BLT mice following HIV infection, whereas the levels of these markers on $CD4^+$ T cells remained unchanged. The percentage of $CD8^+$ T cells expressing perforin, a critical component of effector cytolytic function, increased significantly following the HIV infection of BLT mice, rising from 4.7% ± 0.6% in uninfected mice to 43.1% ± 8.5% in mice 12 weeks p.i. (Fig. 7G).

Humoral immune response to HIV infection. To investigate whether HIV-directed humoral immune responses developed in infected BLT mice, we performed Western blot analyses to detect human HIV-specific antibodies (IgM, IgG, or IgA) at different time points following infection (Fig. 8). No responses were detected in mice infected for 5 weeks or fewer ($n = 10$). At 6 weeks p.i., one mouse out of five tested had equivocally positive antibody responses. At 10 weeks p.i., however, 6 out of 10 mice had definitively positive responses, and 1 mouse had an equivocal response. After 12 or more weeks p.i., all mice tested had Western blots that were definitively positive for the presence of human HIV-specific antibodies ($n = 9$), demonstrating that B cells in BLT mice were able to mount robust virus-specific antibody responses. These responses took longer to develop in HIV-infected BLT mice than in adult human HIV infection, possibly reflecting the immaturity of the human immune systems of these mice initially following reconstitution.

T-cell immune responses to HIV infection. To investigate whether HIV-directed cellular immune responses developed in infected BLT mice, we performed IFN-γ-based ELISPOT analyses at different time points following HIV infection. Cellular immune responses to HIV peptides were detected as early as 3 weeks p.i., when mononuclear cells were expanded nonspecifically in vitro (data not shown). Direct ex vivo responses, however, were not detected in mice tested earlier than 9 weeks p.i. ($n = 4$). At later time points following infection (9 to 18 weeks p.i.), four of six mice tested had positive ELISPOT responses (Fig. 9A, B). These four mice were reconstituted from two separate human tissue donors. Gag- and Nef-derived peptides were the most frequently targeted, as is the case in HIV infection in humans (20). In contrast, all five uninfected mice that were tested had no detectable ELISPOT responses to HIV peptides (Fig. 9A). When sufficient numbers of mononuclear cells were available, we performed intracellular cytokine staining (ICS) assays to confirm positive ELISPOT results and to determine the contribution of $CD4^+$ and $CD8^+$ T cells to these responses. Using autologous HIV_{ADA} peptide pools for Gag and Nef to stimulate cells, both $CD4^+$ and $CD8^+$ T-cell-mediated responses were identified (Fig. 9C). The reconstituted human immune system of one BLT mouse that demonstrated strong ELISPOT responses to Gag-derived overlapping peptides expressed the major histocompatibility complex class I allele HLA-A*0201. Subsequent ICS assays showed that this Gag-directed $CD8^+$ T-cell response was directed largely to the immunodominant epitope SLYNTVATL

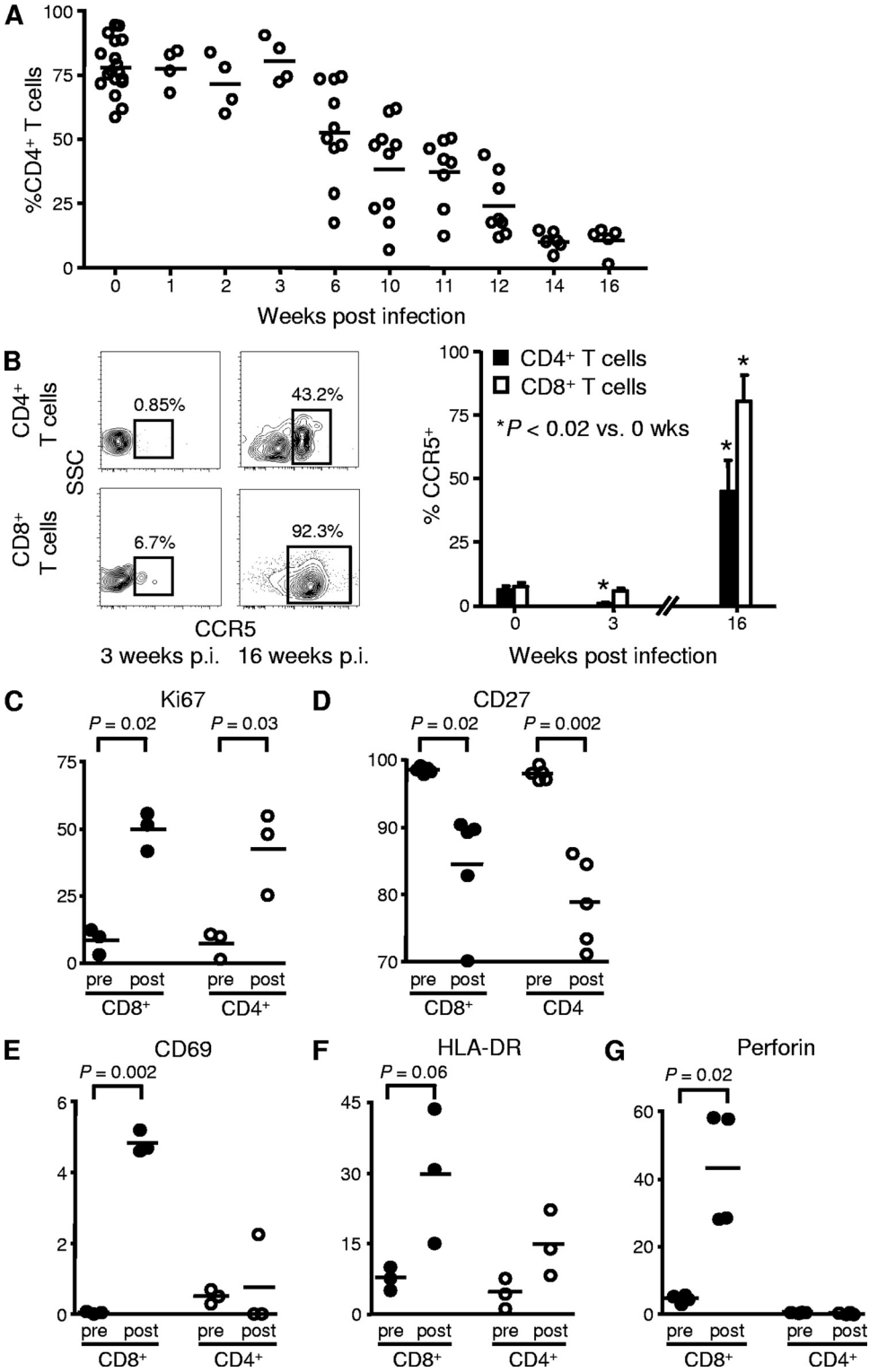

FIG. 7. $CD4^+$ T-cell depletion and immune activation in HIV-infected BLT mice. (A) Percentages of $CD3^+$ T cells in the blood of BLT mice that were $CD4^+$ T cells following infection with 75,000 $TCID_{50}$ of HIV_{ADA}. Each circle represents one mouse; means are shown as solid lines. (B) Percentages of $CD4^+$ and $CD8^+$ T cells in the blood of humanized BLT mice that were $CCR5^+$ following infection with 75,000 $TCID_{50}$ of HIV_{ADA}. Representative flow cytometry plots demonstrate the CCR5 expression of $CD4^+$ and $CD8^+$ T cells at 3 and 16 weeks (wks) p.i. Numbers in the plots represent the percentages of cells contained in the indicated gates. Data presented in the accompanying bar graph represent mean values ± standard errors for three to six mice at each time point. SSC, side scatter. (C to G) The expression levels of multiple activation markers by $CD8^+$ (closed circles) and $CD4^+$ T cells (open circles) were assessed by flow cytometry in two matched blood samples obtained from the same BLT mice, the first obtained pre-HIV infection (pre) and the second 12 weeks p.i. with 75,000 $TCID_{50}$ HIV_{ADA} (post). Each circle represents one mouse; means are shown as solid lines. *P* values, as determined by paired Student's *t* tests, are shown for statistically significant comparisons and those comparisons approaching statistical significance.

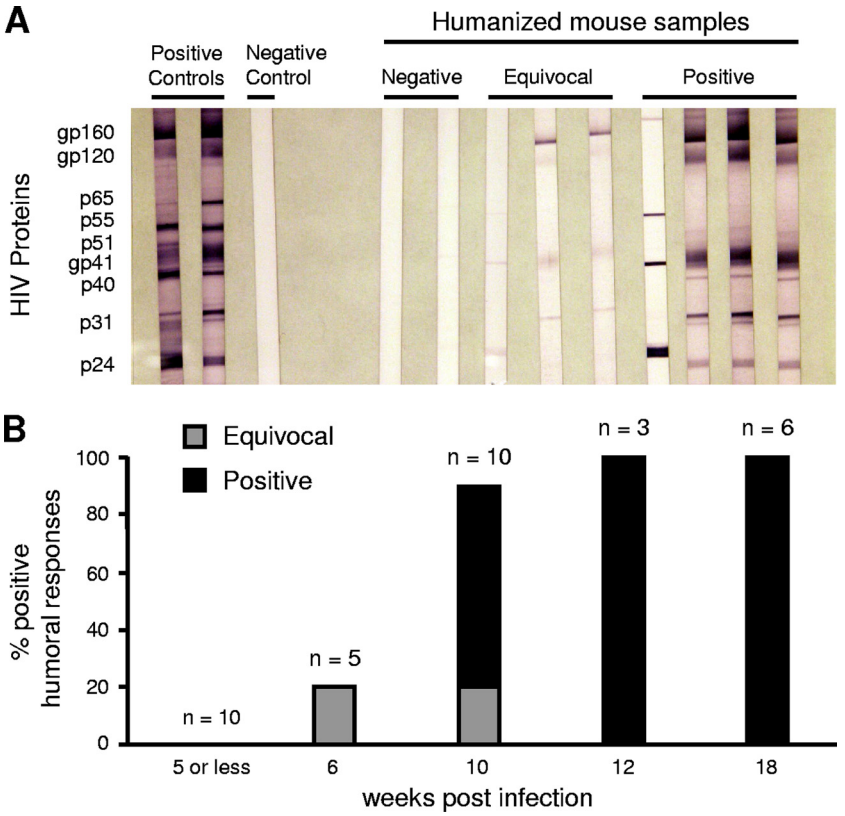

FIG. 8. HIV-specific humoral immune responses in HIV-infected BLT mice. (A) Western blot analyses are shown for representative HIV-infected BLT mice with negative ($n = 2$), equivocal ($n = 3$), and positive ($n = 4$) HIV-specific antibody responses in plasma. Positive and negative human controls are shown for comparison. (B) Time course of the development of HIV-specific antibodies in BLT mice following infection. The total number of mice tested at each time point is indicated.

(SL9), which is located in HIV Gag p17 (Fig. 9C). As with the ELISPOT assays, uninfected mice had no detectable ICS responses to HIV peptides (Fig. 9D). These results demonstrate that BLT mice are able to generate robust, broadly directed HIV-specific $CD8^+$ and $CD4^+$ T-cell responses.

T-cell PD-1 upregulation following HIV infection. Despite the generation of robust HIV-specific immune responses in BLT mice, viral loads remained elevated, raising the possibility that these responses are dysfunctional. The increased expression of the inhibitory receptor PD-1 on functionally exhausted T cells has been implicated in the dysfunction of anti-HIV immune responses observed in chronic human HIV infection (12, 48, 62). PD-1 blockade during chronic SIV infection in rhesus macaques recently was shown to enhance T-cell immunity and was associated with reductions in plasma viral load and prolonged survival (64). We therefore examined the PD-1 expression of circulating T cells in BLT mice before and after HIV infection. We found that HIV infection increased the percentage of T cells expressing PD-1 as well as the mean fluorescence intensity of the PD-1-positive population, as demonstrated by $CD8^+$ cells from a representative mouse in Fig. 10A. The percentages of $CD8^+$ T cells that expressed PD-1 were significantly higher in infected mice than in uninfected mice as early as 2 weeks p.i. ($21.2\% \pm 3.3\%$ and $8.8 \pm 0.9\%$; $n = 8$; $P = 0.002$ at 2 versus 0 weeks p.i.) (Fig. 10B). $CD4^+$ T cells upregulated PD-1 expression more slowly, with percentages of $CD4^+$ T cells that expressed PD-1 in infected mice becoming significantly higher than percentages in uninfected mice at week 12 p.i. ($41.6\% \pm 8.6\%$ and $8.4\% \pm 1.8\%$; $n = 8$; $P = 0.002$ at 12 versus 0 weeks p.i.) (Fig. 10B). Interestingly, the high percentages of total $CD8^+$ and $CD4^+$ T cells that expressed PD-1 in HIV-infected BLT mice have been observed for HIV-specific but not total $CD8^+$ and $CD4^+$ T cells in HIV-infected persons (12, 48, 62), suggesting that the nonspecific immune activation observed in BLT mice following HIV infection also contributed to increased PD-1 expression. In contrast to those of infected mice, the percentages of T cells expressing PD-1 in uninfected mice remained below 10% during the course of several months (data not shown). We found significant inverse correlations between the $CD4^+$ T-cell percentages in the circulation of HIV-infected BLT mice and the percentages of both their $CD8^+$ ($r = -0.8684$; $P < 0.0001$) and their $CD4^+$ T cells ($r = -0.7905$; $P < 0.0001$) that expressed PD-1 (Fig. 10C). Although plasma viremia levels demonstrated only modest declines from peak levels within individual infected mice, we found significant positive correlations between plasma viremia levels in different HIV-infected BLT mice and the percentages of their $CD8^+$ ($r = 0.3575$; $P = 0.04$) and $CD4^+$ T cells ($r = 0.3595$; $P = 0.04$) that expressed PD-1 (Fig. 10D). These data for BLT mice mirror the findings in human HIV infection that T-cell PD-1 expression correlates with two

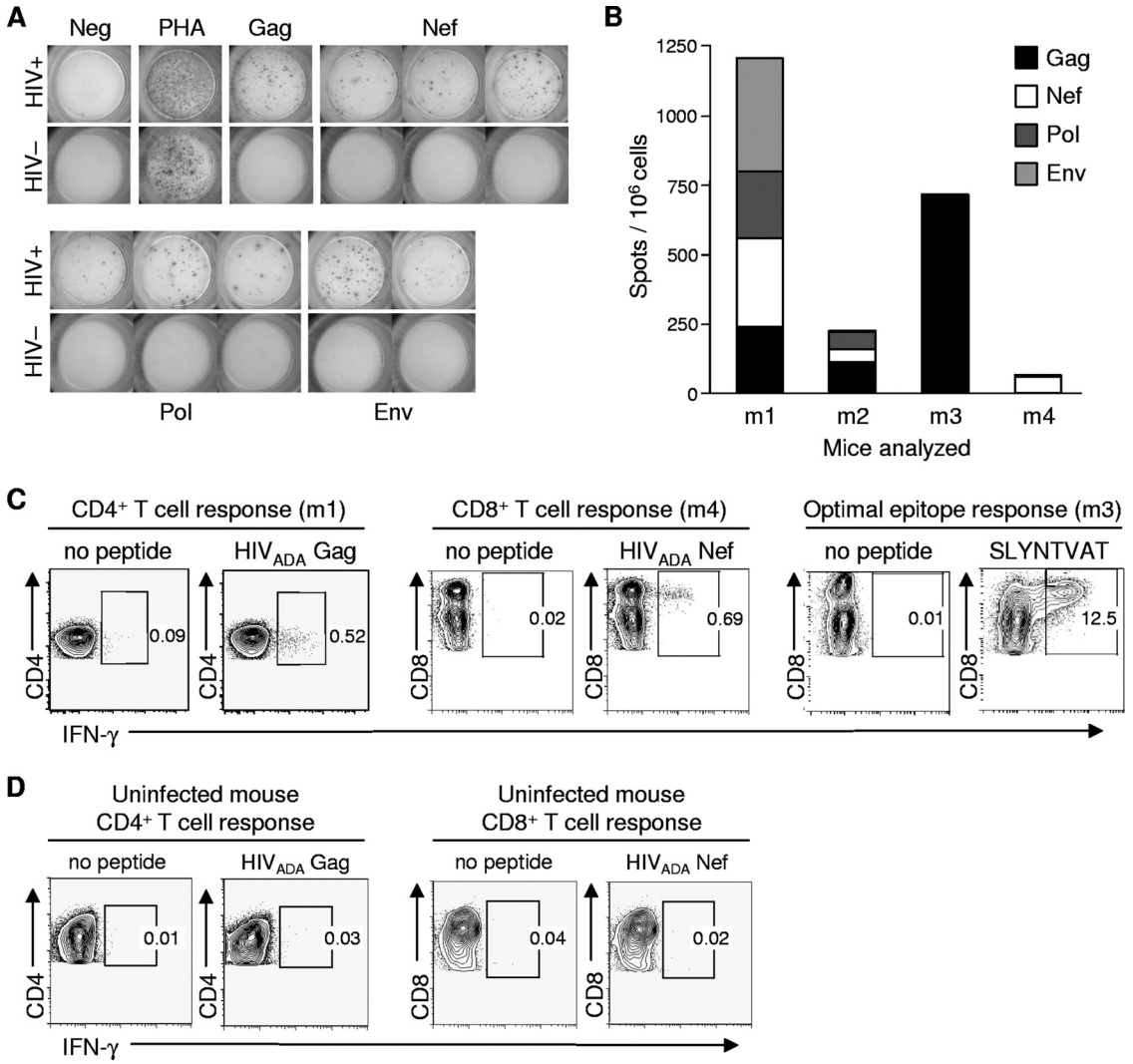

FIG. 9. HIV-specific cellular immune responses in HIV-infected BLT mice. (A) Representative ELISPOT data demonstrating HIV peptide-induced IFN-γ secretion by BLT mouse mononuclear cells pooled from the blood, spleen, and LN. The top panels show data using cells from an HIV-infected BLT mouse 10 weeks following infection; the bottom panels show data using cells from an uninfected BLT mouse. Cells were stimulated with overlapping 18-mer peptide pools spanning the HIV proteome, and positive responses to the indicated HIV proteins are shown, in addition to the no-peptide negative control and the phytohemagglutinin-positive control. (B) Analysis of ELISPOT data showing the magnitude and breadth of anti-HIV T-cell responses in four HIV-infected BLT mice (designated mouse 1 [m1], m2, m3, and m4). (C) Confirmation of positive ELISPOT responses by ICS of BLT mouse mononuclear cells for IFN-γ production following autologous peptide pool stimulation. Representative contour plots show both $CD4^+$ and $CD8^+$ T-cell HIV-specific responses. Numbers in the panels represent percentages of cells contained in the indicated gates. A mouse reconstituted with HLA-A2-expressing human tissue (m3) was found to generate a robust T-cell response directed against the A2-restricted Gag epitope SLYNTVATL (right panels). (D) Uninfected BLT mice did not demonstrate any T-cell responses to HIV peptides.

strong predictors of disease progression: declining $CD4^+$ counts and increasing viral loads (12, 62).

DISCUSSION

We confirmed that the generation of BLT mice by the cotransplantation of human fetal thymic and liver tissues and autologous $CD34^+$ FLC into immunodeficient NOD/SCID mice produces stable high-level engraftment of human immune cells, characterized by the presence of human progenitor cells in their bone marrow and thymic grafts and differentiated T cells, B cells, DCs, and monocytes/macrophages in their peripheral blood and tissues. A robust population of true hematopoietic stem cells was seen in BLT mouse bone marrow. The human $CD4^+$ and $CD8^+$ T cells present in the spleens of BLT mice demonstrated a naïve phenotype. Although human B-cell development in the bone marrow and spleens of BLT mice demonstrated some skewing toward immature cells, mature follicular B cells, marginal-zone B cells, and plasmablasts all were present. Both human mDCs and pDCs were present in the blood and spleens of BLT mice, and both human classical monocytes and more mature macrophage-like monocytes were identified in their lungs. Immunostaining also demonstrated the reconstitution of the gastrointestinal tracts of BLT mice with human T cells, B cells, and macrophages.

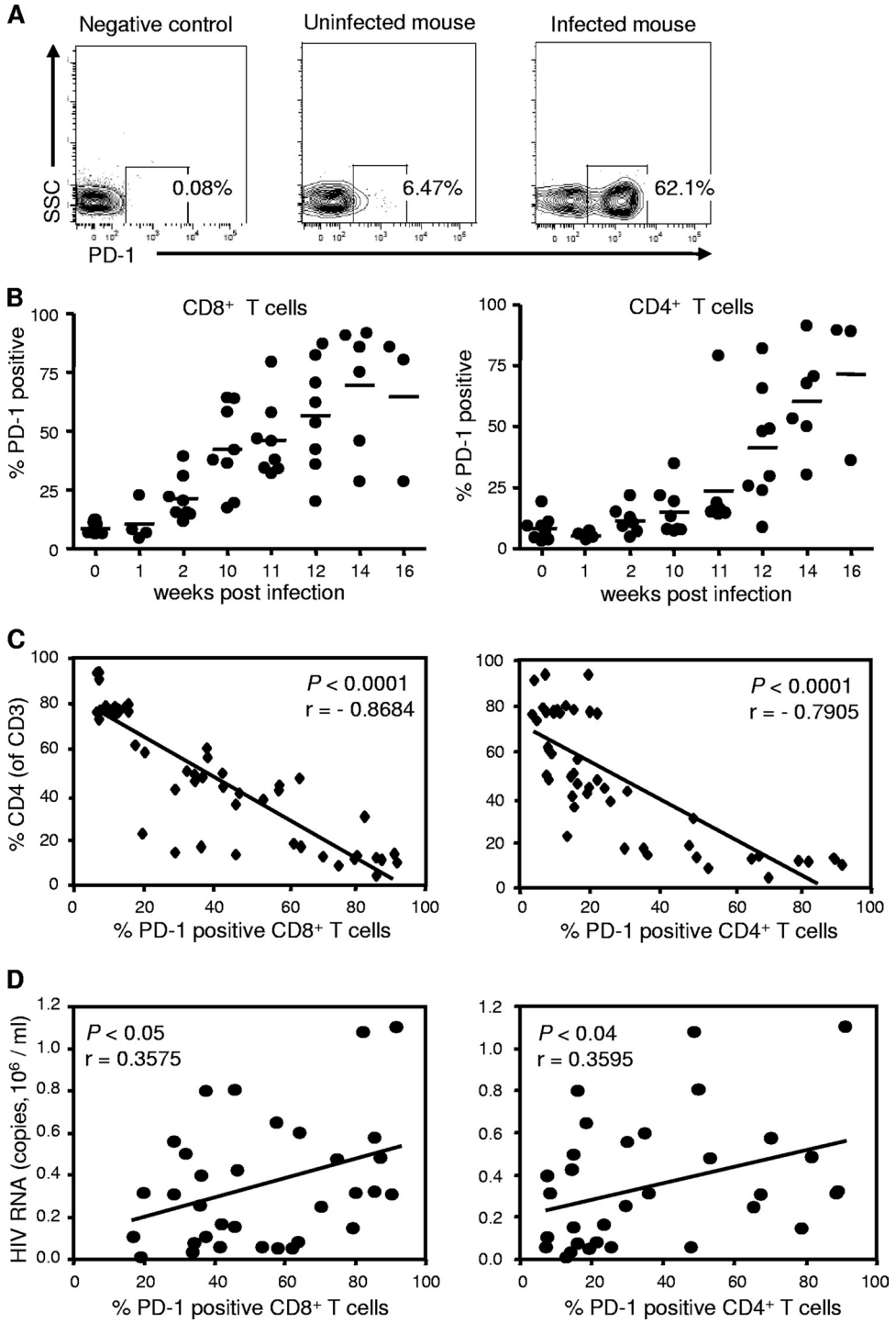

FIG. 10. T-cell PD-1 upregulation in HIV-infected BLT mice. (A) PD-1 expression by $CD8^+$ T cells from representative uninfected and infected BLT mice (12 weeks p.i.). SSC, side scatter. (B) Percentages of $CD8^+$ and $CD4^+$ T cells in BLT mice expressing PD-1 at the indicated time points following infection with 75,000 $TCID_{50}$ HIV_{ADA}. Each circle represents an individual mouse; means are shown as solid lines. (C) Correlations between the percentages of $CD8^+$ and $CD4^+$ T cells expressing PD-1, and the percentages of peripheral blood T cells that were $CD4^+$ T cells, in BLT mice following infection with 75,000 $TCID_{50}$ HIV_{ADA}. (D) Correlations between the percentages of $CD8^+$ and $CD4^+$ T cells expressing PD-1, and plasma viral loads, in BLT mice following infection with 75,000 $TCID_{50}$ HIV_{ADA}.

Following this human immune reconstitution, we found that BLT mice sustained high levels of HIV infection for at least several months, with viral dissemination to lymphoid tissues, $CD4^+$ T-cell depletion, and immune activation. We then characterized the robust emergence of HIV-specific humoral and cellular human adaptive immune responses in BLT mice following HIV infection, although these responses took longer to develop than has been reported in adult humans (1).

Multiple investigators have reported similar findings regarding the extent and duration of HIV infection in other humanized mouse models, including cord blood cell- or fetal liver stem cell-transplanted Rag2$^{-/-}$ $\gamma_c^{-/-}$ mice (2–4, 24, 29, 67) and cord blood cell-transplanted NOD/SCID/$\gamma_c^{-/-}$ mice (65), and sustained HIV infection previously has been demonstrated in BLT mice (13, 59). Immune responses against non-HIV antigens and/or pathogens have been reported in humanized mice as well. Cord blood cell-transplanted Rag2$^{-/-}$ $\gamma_c^{-/-}$ mice have demonstrated anti-tetanus toxoid and anti-*Haemophilus influenzae* antibody production as well as Epstein-Barr virus-induced CD8$^+$ T-cell proliferation (24, 61); Rag2$^{-/-}$ $\gamma_c^{-/-}$ mice reconstituted with human fetal liver CD34$^+$ cells have generated anti-dengue virus antibodies that demonstrated both class switching and neutralizing capacity (32). BLT mice previously have demonstrated the expansion of human $\nu\beta2$ T-cell receptor-positive T cells induced by toxic shock syndrome toxin and T-cell IFN-γ production induced by Epstein-Barr virus (41), and we previously reported the ability of these humanized mice to develop antigen-specific, T-cell-dependent antibody responses after in vivo immunization with the T-dependent antigen 2,4-dinitrophenyl hapten-keyhole limpet hemocyanin (DNP23-KLH) (60).

However, robust human anti-HIV adaptive immune responses in humanized mice have not been reported previously. Only two prior reports have documented HIV-specific B-cell responses, and these have been in the minority of the mice investigated: HIV-specific antibodies were present in one of 25 HIV-infected human cord blood cell-transplanted Rag2$^{-/-}$ $\gamma_c^{-/-}$ mice (2) and in 3 of 14 HIV-infected cord blood cell-transplanted NOD/SCID/$\gamma_c^{-/-}$ mice (65). The cord blood cell-transplanted Rag2$^{-/-}$ $\gamma_c^{-/-}$ mice noted above to produce *Haemophilus influenzae* type b-specific antibodies following *H. influenzae* type b vaccination failed to produce HIV-specific antibodies following HIV infection (24). In contrast, we demonstrated the appearance of robust HIV-specific antibody responses in all humanized mice after 12 weeks of infection. In the case of cell-mediated immunity, whereas HIV-specific T-cell responses have not been reported previously for humanized mice, we have demonstrated the appearance of robust anti-HIV CD4$^+$ and CD8$^+$ T-cell responses in the majority of our mice tested at 9 weeks or longer postinfection. We hypothesize that the development of HIV-specific CD4$^+$ and CD8$^+$ T-cell responses in HIV-infected BLT mice underscores the importance of providing autologous human thymic tissue for the functional development of human T cells capable of responding to HIV in vivo. The development of more robust HIV-specific antibody responses in BLT mice than have been described previously suggests that the improved function of human T cells in the BLT model contributes to the improved generation of B-cell responses as well. The human anti-HIV cellular and humoral immune responses that we have documented in BLT mice suggest that this model of HIV infection is able to test human immune responses to HIV vaccines.

We did not determine whether the HIV-specific antibodies that were generated in HIV-infected BLT mice demonstrated class switching from IgM to IgG, and if so, which IgG subtype(s) were present, as the detection antibody used in the Western blot analyses did not distinguish between IgG, IgM, and IgA antibodies. We have demonstrated the occurrence of antibody class switching in BLT mice in prior studies of non-HIV-infected mice (33, 60), providing further evidence of T-cell functionality in these humanized mice. We found that the immunization of BLT mice with the T-cell-dependent antigen DNP23-KLH produced human DNP-specific antibodies that demonstrated class switching to IgG. The analysis of isotype subclasses revealed that DNP-specific IgG antibodies in immunized BLT mice mainly were IgG1 and IgG2, similarly to those of antibody responses in humans after KLH immunization (5). In contrast, the DNP-KLH immunization of NOD/SCID/$\gamma_c^{-/-}$ mice transplanted with human umbilical cord blood, bone marrow, or mobilized peripheral blood CD34$^+$ cells but not with fetal thymic tissue previously has been reported to produce antigen-specific human IgM, but not IgG, responses (38). The isotypes of HIV-specific antibodies generated in our BLT mice, as well as their neutralizing capacity, will be investigated in follow-up studies.

In addition to the generation of virus-specific immune responses, HIV infection in humans and SIV infection in macaques produce generalized immune activation (15, 16, 58), and we now have demonstrated that this aspect of HIV infection can be modeled in humanized mice as well. Following the HIV infection of BLT mice, we observed increased CD8$^+$ and CD4$^+$ T-cell turnover, as indicated by high levels of Ki-67 expression, as well as the increased expression of perforin by CD8$^+$ T cells, similarly to human HIV infection (28, 51). Analyses of other cell surface markers also were consistent with increased T-cell activation following the HIV infection of BLT mice: both CD4$^+$ and CD8$^+$ T cells demonstrated decreased CD27 expression and increased CCR5 expression after HIV infection. In contrast, CD69 and HLA-DR were upregulated significantly in CD8$^+$ T cells but not CD4$^+$ T cells. One possible explanation for this finding of more activated CD8$^+$ than CD4$^+$ T cells is the preferential infection and elimination of the most activated CD4$^+$ T lymphocytes by HIV.

Following infection with 75,000 $TCID_{50}$ HIV_{ADA}, BLT mice demonstrated peak plasma viremia exceeding 1.5 million copies/ml at 6 weeks p.i., with only a slow decline in mean viral load noted during the ensuing months. These viral kinetics are similar to those seen in the HIV infection of other humanized mouse models (2, 65) and are reminiscent of human perinatal HIV infection, in which copy numbers of HIV-1 RNA rise from generally low values (<10,000 copies per ml) at birth to high values (>100,000 copies per ml) within the first 2 months of life and then fall very slowly during the next 24 months (55). This slow decline in the viral load of infected infants contrasts sharply with the rapid decline in the viral load that occurs in most adults following primary HIV-1 infection, usually to a set point at least one log lower than the peak level, and suggests that the immature neonatal immune system is unable to contain HIV replication to the same degree as the mature adult immune system (18). The similarly slow decline in viral load observed in our mouse model suggests that the human immune system in these mice more closely resembles that of children than of adults.

The persistence of high viral loads with only modest declines from the peak plasma viremia noted above occurred despite the expansion of HIV-specific T cells in most infected mice, raising the possibility that these cells are dysfunctional. Since the PD-1 receptor has been implicated in impaired T-cell func-

tion in human HIV infection (12, 48, 62), we determined T-cell PD-1 receptor expression before and after HIV infection in BLT mice. We found that PD-1 levels rose on both $CD4^+$ and $CD8^+$ T cells over time following HIV infection in these mice, similarly to what is seen in human infection. Furthermore, PD-1 expression correlated strongly with viral load and inversely with the percentage of circulating $CD4^+$ T cells, two strong predictors of disease progression. Although these data do not establish whether there is a causal relationship between increased PD-1 expression and the dysfunction of human HIV-specific T cells in vivo, they do demonstrate that humanized BLT mice will support experiments designed to address this question. Such experiments recently have been reported for rhesus macaques, in which PD-1 blockade during SIV infection enhanced macaque T-cell immunity and was associated with reductions in plasma viral load and prolonged survival (64).

The inability of BLT mice to control HIV replication after the direct injection of high doses of laboratory strains, however, does not necessarily indicate generalized dysfunction of the human immune responses generated in these animals. In prior studies of non-HIV-infected mice, we demonstrated the improved function of the reconstituted human immune system in BLT mice compared to that of NOD/SCID mice reconstituted with thymic and liver tissues but not with purified $CD34^+$ FLC (33). We found that BLT mice were able to reject porcine skin xenografts, which requires the presentation of graft antigens to T cells as well as T-cell activation, expansion, and trafficking to the graft, whereas NOD/SCID mice reconstituted with thymic and liver tissues but not FLC were unable to reject these xenografts. Although these experiments demonstrated a substantially improved function of human immune cells in non-HIV-infected BLT mice, additional studies will be required to further define the immune capabilities of these mice. If immune dysfunction is present in HIV-infected BLT mice, it will be important to determine whether such dysfunction occurs specifically as a result of HIV infection or occurs intrinsically in these mice prior to infection.

As we have shown, humanized BLT mice demonstrated high levels of disseminated HIV infection with the attendant generation of robust virus-specific cellular and humoral human immune responses, suggesting that these mice are able to provide a new platform to test human immune responses to HIV vaccines. The HIV infection of BLT mice also resulted in generalized immune activation and the upregulation of T-cell PD-1 expression. These additional responses of human immune cells to HIV infection in BLT mice suggest that these mice also provide a valuable model to investigate HIV pathogenesis and host immunity in vivo and to evaluate new immunomodulatory therapeutic strategies such as blockade of the PD-1 pathway.

ACKNOWLEDGMENTS

This work was supported by a Harvard University CFAR (HU CFAR) Scholar Award and an HU CFAR Collaborative Feasibility Study Award to A.T. and by National Institutes of Health grants K08 AI058857 to D.B., R01 A1067077 to C.B., AI064930 and AI069458 to S.P., P30 AI060354 to B.W., P51 RR00168 and T32 RR07000 to S.V.W., and P01 AI078897 (Project 4) to A.L.

We thank Leonard D. Shultz for kindly providing the NOD/SCID/$\gamma_c^{-/-}$ mice and David Scadden and Nancy L. Harris for providing human tissue samples. We also thank Patricia Della-Pella for her excellent technical assistance with HIV Gag-p24 immunohistochemistry, Kari Hartman and Leah Whiteman for their excellent technical assistance with ELISPOT assays, and Suzan Lazo-Kallanian, John Daley, and Michelle Connole for help with flow cytometry.

We have no conflicting financial interests.

REFERENCES

1. **Altfeld, M., E. S. Rosenberg, R. Shankarappa, J. S. Mukherjee, F. M. Hecht, R. L. Eldridge, M. M. Addo, S. H. Poon, M. N. Phillips, G. K. Robbins, P. E. Sax, S. Boswell, J. O. Kahn, C. Brander, P. J. Goulder, J. A. Levy, J. I. Mullins, and B. D. Walker.** 2001. Cellular immune responses and viral diversity in individuals treated during acute and early HIV-1 infection. J. Exp. Med. **193:**169–180.
2. **Baenziger, S., R. Tussiwand, E. Schlaepfer, L. Mazzucchelli, M. Heikenwalder, M. O. Kurrer, S. Behnke, J. Frey, A. Oxenius, H. Joller, A. Aguzzi, M. G. Manz, and R. F. Speck.** 2006. Disseminated and sustained HIV infection in $CD34^+$ cord blood cell-transplanted $Rag2^{-/-}$ $\gamma_c^{-/-}$ mice. Proc. Natl. Acad. Sci. USA **103:**15951–15956.
3. **Berges, B. K., S. R. Akkina, J. M. Folkvord, E. Connick, and R. Akkina.** 2008. Mucosal transmission of R5 and X4 tropic HIV-1 via vaginal and rectal routes in humanized $Rag2^{-/-}$ $\gamma_c^{-/-}$ (RAG-hu) mice. Virology **373:**342–351.
4. **Berges, B. K., W. H. Wheat, B. E. Palmer, E. Connick, and R. Akkina.** 2006. HIV-1 infection and CD4 T-cell depletion in the humanized $Rag2^{-/-}$ $\gamma_c^{-/-}$ (RAG-hu) mouse model. Retrovirology **3:**76.
5. **Bird, P., J. E. Calvert, and P. L. Amlot.** 1990. Distinctive development of IgG4 subclass antibodies in the primary and secondary responses to keyhole limpet haemocyanin in man. Immunology **69:**355–360.
6. **Bleesing, J. J., and T. A. Fleisher.** 2003. Human B cells express a CD45 isoform that is similar to murine B220 and is downregulated with acquisition of the memory B-cell marker CD27. Cytometry B Clin. Cytom **51:**1–8.
7. **Browning, J., J. W. Horner, M. Pettoello-Mantovani, C. Raker, S. Yurasov, R. A. DePinho, and H. Goldstein.** 1997. Mice transgenic for human CD4 and CCR5 are susceptible to HIV infection. Proc. Natl. Acad. Sci. USA **94:**14637–14641.
8. **Cariappa, A., C. Boboila, S. T. Moran, H. Liu, H. N. Shi, and S. Pillai.** 2007. The recirculating B cell pool contains two functionally distinct, long-lived, posttransitional, follicular B cell populations. J. Immunol. **179:**2270–2281.
9. **Cariappa, A., C. Chase, H. Liu, P. Russell, and S. Pillai.** 2007. Naive recirculating B cells mature simultaneously in the spleen and bone marrow. Blood **109:**2339–2345.
10. **Cariappa, A., I. B. Mazo, C. Chase, H. N. Shi, H. Liu, Q. Li, H. Rose, H. Leung, B. J. Cherayil, P. Russell, U. von Andrian, and S. Pillai.** 2005. Perisinusoidal B cells in the bone marrow participate in T-independent responses to blood-borne microbes. Immunity **23:**397–407.
11. **Cariappa, A., H. Takematsu, H. Liu, S. Diaz, K. Haider, C. Boboila, G. Kalloo, M. Connole, H. N. Shi, N. Varki, A. Varki, and S. Pillai.** 2009. B cell antigen receptor signal strength and peripheral B cell development are regulated by a 9-O-acetyl sialic acid esterase. J. Exp. Med. **206:**125–138.
12. **Day, C. L., D. E. Kaufmann, P. Kiepiela, J. A. Brown, E. S. Moodley, S. Reddy, E. W. Mackey, J. D. Miller, A. J. Leslie, C. DePierres, Z. Mncube, J. Duraiswamy, B. Zhu, Q. Eichbaum, M. Altfeld, E. J. Wherry, H. M. Coovadia, P. J. Goulder, P. Klenerman, R. Ahmed, G. J. Freeman, and B. D. Walker.** 2006. PD-1 expression on HIV-specific T cells is associated with T-cell exhaustion and disease progression. Nature **443:**350–354.
13. **Denton, P. W., J. D. Estes, Z. Sun, F. A. Othieno, B. L. Wei, A. K. Wege, D. A. Powell, D. Payne, A. T. Haase, and J. V. Garcia.** 2008. Antiretroviral preexposure prophylaxis prevents vaginal transmission of HIV-1 in humanized BLT mice. PLoS Med. **5:**e16.
14. **Dorfman, D. M., J. A. Brown, A. Shahsafaei, and G. J. Freeman.** 2006. Programmed death-1 (PD-1) is a marker of germinal center-associated T cells and angioimmunoblastic T-cell lymphoma. Am. J. Surg. Pathol. **30:**802–810.
15. **Douek, D. C., L. J. Picker, and R. A. Koup.** 2003. T cell dynamics in HIV-1 infection. Annu. Rev. Immunol. **21:**265–304.
16. **Douek, D. C., M. Roederer, and R. A. Koup.** 2009. Emerging concepts in the immunopathogenesis of AIDS. Annu. Rev. Med. **60:**471–484.
17. **Draenert, R., C. L. Verrill, Y. Tang, T. M. Allen, A. G. Wurcel, M. Boczanowski, A. Lechner, A. Y. Kim, T. Suscovich, N. V. Brown, M. M. Addo, and B. D. Walker.** 2004. Persistent recognition of autologous virus by high-avidity CD8 T cells in chronic, progressive human immunodeficiency virus type 1 infection. J. Virol. **78:**630–641.
18. **Feeney, M. E.** 2004. HIV and children: the developing immune system fights back. West Indian Med. J. **53:**359–362.
19. **Flores, K. G., J. Li, G. D. Sempowski, B. F. Haynes, and L. P. Hale.** 1999. Analysis of the human thymic perivascular space during aging. J. Clin. Investig. **104:**1031–1039.
20. **Frahm, N., B. T. Korber, C. M. Adams, J. J. Szinger, R. Draenert, M. M. Addo, M. E. Feeney, K. Yusim, K. Sango, N. V. Brown, D. SenGupta, A. Piechocka-Trocha, T. Simonis, F. M. Marincola, A. G. Wurcel, D. R. Stone, C. J. Russell, P. Adolf, D. Cohen, T. Roach, A. StJohn, A. Khatri, K. Davis, J. Mullins, P. J. Goulder, B. D. Walker, and C. Brander.** 2004. Consistent

cytotoxic-T-lymphocyte targeting of immunodominant regions in human immunodeficiency virus across multiple ethnicities. J. Virol. **78:**2187–2200.

21. **Gajkowska, A., T. Oldak, M. Jastrzewska, E. K. Machaj, J. Walewski, E. Kraszewska, and Z. Pojda.** 2006. Flow cytometric enumeration of CD34+ hematopoietic stem and progenitor cells in leukapheresis product and bone marrow for clinical transplantation: a comparison of three methods. Folia Histochem. Cytobiol. **44:**53–60.
22. **Giannelli, S., A. Taddeo, P. Presicce, M. L. Villa, and S. Della Bella.** 2008. A six-color flow cytometric assay for the analysis of peripheral blood dendritic cells. Cytometry B Clin. Cytom. **74:**349–355.
23. **Gorantla, S., K. Santos, V. Meyer, S. Dewhurst, W. J. Bowers, H. J. Federoff, H. E. Gendelman, and L. Poluektova.** 2005. Human dendritic cells transduced with herpes simplex virus amplicons encoding human immunodeficiency virus type 1 (HIV-1) gp120 elicit adaptive immune responses from human cells engrafted into NOD/SCID mice and confer partial protection against HIV-1 challenge. J. Virol. **79:**2124–2132.
24. **Gorantla, S., H. Sneller, L. Walters, J. G. Sharp, S. J. Pirruccello, J. T. West, C. Wood, S. Dewhurst, H. E. Gendelman, and L. Poluektova.** 2007. Human immunodeficiency virus type 1 pathobiology studied in humanized BALB/c-Rag2$^{-/-}$ $\gamma_c^{-/-}$ mice. J. Virol. **81:**2700–2712.
25. **Grage-Griebenow, E., H. D. Flad, and M. Ernst.** 2001. Heterogeneity of human peripheral blood monocyte subsets. J. Leukoc. Biol. **69:**11–20.
26. **Ishikawa, F., M. Yasukawa, B. Lyons, S. Yoshida, T. Miyamoto, G. Yoshimoto, T. Watanabe, K. Akashi, L. D. Shultz, and M. Harada.** 2005. Development of functional human blood and immune systems in NOD/SCID/IL2 receptor γ chain^{null} mice. Blood **106:**1565–1573.
27. **Ito, M., H. Hiramatsu, K. Kobayashi, K. Suzue, M. Kawahata, K. Hioki, Y. Ueyama, Y. Koyanagi, K. Sugamura, K. Tsuji, T. Heike, and T. Nakahata.** 2002. NOD/SCID/γ_c^{null} mouse: an excellent recipient mouse model for engraftment of human cells. Blood **100:**3175–3182.
28. **Jansen, C. A., E. Piriou, C. Bronke, J. Vingerhoed, S. Kostense, D. van Baarle, and F. Miedema.** 2004. Characterization of virus-specific CD8$^+$ effector T cells in the course of HIV-1 infection: longitudinal analyses in slow and rapid progressors. Clin. Immunol. **113:**299–309.
29. **Jiang, Q., L. Zhang, R. Wang, J. Jeffrey, M. L. Washburn, D. Brouwer, S. Barbour, G. I. Kovalev, D. Unutmaz, and L. Su.** 2008. FoxP3$^+$CD4$^+$ Treg cells play an important role in acute HIV-1 infection in humanized rag2$^{-/-}$ γC$^{-/-}$ mice in vivo. Blood **112:**2858–2868.
30. **Koff, W. C., P. R. Johnson, D. I. Watkins, D. R. Burton, J. D. Lifson, K. J. Hasenkrug, A. B. McDermott, A. Schultz, T. J. Zamb, R. Boyle, and R. C. Desrosiers.** 2006. HIV vaccine design: insights from live attenuated SIV vaccines. Nat. Immunol. **7:**19–23.
31. **Kumar, P., H. S. Ban, S. S. Kim, H. Wu, T. Pearson, D. L. Greiner, A. Laouar, J. Yao, V. Haridas, K. Habiro, Y. G. Yang, J. H. Jeong, K. Y. Lee, Y. H. Kim, S. W. Kim, M. Peipp, G. H. Fey, N. Manjunath, L. D. Shultz, S. K. Lee, and P. Shankar.** 2008. T cell-specific siRNA delivery suppresses HIV-1 infection in humanized mice. Cell **134:**577–586.
32. **Kuruvilla, J. G., R. M. Troyer, S. Devi, and R. Akkina.** 2007. Dengue virus infection and immune response in humanized RAG2$^{-/-}$ $\gamma_c^{-/-}$ (RAG-hu) mice. Virology **369:**143–152.
33. **Lan, P., N. Tonomura, A. Shimizu, S. Wang, and Y. G. Yang.** 2006. Reconstitution of a functional human immune system in immunodeficient mice through combined human fetal thymus/liver and CD34$^+$ cell transplantation. Blood **108:**487–492.
34. **Lan, P., L. Wang, B. Diouf, H. Eguchi, H. Su, R. Bronson, D. H. Sachs, M. Sykes, and Y. G. Yang.** 2004. Induction of human T-cell tolerance to porcine xenoantigens through mixed hematopoietic chimerism. Blood **103:**3964–3969.
35. **LeBien, T. W., B. Wormann, J. G. Villablanca, C. L. Law, L. M. Steinberg, V. O. Shah, and M. R. Loken.** 1990. Multiparameter flow cytometric analysis of human fetal bone marrow B cells. Leukemia **4:**354–358.
36. **Leuner, S., M. Arland, C. Kahl, K. Jentsch-Ullrich, A. Franke, and H. G. Hoffkes.** 1998. Enumeration of CD34-positive hematopoietic progenitor cells by flow cytometry: comparison of a volumetric assay and the ISHAGE gating strategy. Bone Marrow Transplant. **22:**699–706.
37. **Lorès, P., V. Boucher, C. Mackay, M. Pla, H. Von Boehmer, J. Jami, F. Barre-Sinoussi, and J. C. Weill.** 1992. Expression of human CD4 in transgenic mice does not confer sensitivity to human immunodeficiency virus infection. AIDS Res. Hum. Retrovir. **8:**2063–2071.
38. **Matsumura, T., Y. Kametani, K. Ando, Y. Hirano, I. Katano, R. Ito, M. Shiina, H. Tsukamoto, Y. Saito, Y. Tokuda, S. Kato, M. Ito, K. Motoyoshi, and S. Habu.** 2003. Functional CD5$^+$ B cells develop predominantly in the spleen of NOD/SCID/γ_c^{null} (NOG) mice transplanted either with human umbilical cord blood, bone marrow, or mobilized peripheral blood CD34$^+$ cells. Exp. Hematol. **31:**789–797.
39. **McCune, J. M., R. Namikawa, H. Kaneshima, L. D. Shultz, M. Lieberman, and I. L. Weissman.** 1988. The SCID-hu mouse: murine model for the analysis of human hematolymphoid differentiation and function. Science **241:**1632–1639.
40. **McKinney, D. M., D. A. Lewinsohn, S. R. Riddell, P. D. Greenberg, and D. E. Mosier.** 1999. The antiviral activity of HIV-specific CD8$^+$ CTL clones is limited by elimination due to encounter with HIV-infected targets. J. Immunol. **163:**861–867.
41. **Melkus, M. W., J. D. Estes, A. Padgett-Thomas, J. Gatlin, P. W. Denton, F. A. Othieno, A. K. Wege, A. T. Haase, and J. V. Garcia.** 2006. Humanized mice mount specific adaptive and innate immune responses to EBV and TSST-1. Nat. Med. **12:**1316–1322.
42. **Mosier, D. E., R. J. Gulizia, S. M. Baird, and D. B. Wilson.** 1988. Transfer of a functional human immune system to mice with severe combined immunodeficiency. Nature **335:**256–259.
43. **Mosier, D. E., R. J. Gulizia, S. M. Baird, D. B. Wilson, D. H. Spector, and S. A. Spector.** 1991. Human immunodeficiency virus infection of human-PBL-SCID mice. Science **251:**791–794.
44. **Nakata, H., K. Maeda, T. Miyakawa, S. Shibayama, M. Matsuo, Y. Takaoka, M. Ito, Y. Koyanagi, and H. Mitsuya.** 2005. Potent anti-R5 human immunodeficiency virus type 1 effects of a CCR5 antagonist, AK602/ONO4128/GW873140, in a novel human peripheral blood mononuclear cell nonobese diabetic-SCID, interleukin-2 receptor gamma-chain-knocked-out AIDS mouse model. J. Virol. **79:**2087–2096.
45. **Namikawa, R., H. Kaneshima, M. Lieberman, I. L. Weissman, and J. M. McCune.** 1988. Infection of the SCID-hu mouse by HIV-1. Science **242:**1684–1686.
46. **O'Neil, S. P., S. P. Mossman, D. H. Maul, and E. A. Hoover.** 1999. In vivo cell and tissue tropism of SIVsmmPBj14-bcl. 3. AIDS Res. Hum Retrovir. **15:**203–215.
47. **O'Neil, S. P., F. J. Novembre, A. B. Hill, C. Suwyn, C. E. Hart, T. Evans-Strickfaden, D. C. Anderson, J. deRosayro, J. G. Herndon, M. Saucier, and H. M. McClure.** 2000. Progressive infection in a subset of HIV-1-positive chimpanzees. J. Infect. Dis. **182:**1051–1062.
48. **Petrovas, C., J. P. Casazza, J. M. Brenchley, D. A. Price, E. Gostick, W. C. Adams, M. L. Precopio, T. Schacker, M. Roederer, D. C. Douek, and R. A. Koup.** 2006. PD-1 is a regulator of virus-specific CD8$^+$ T cell survival in HIV infection. J. Exp. Med. **203:**2281–2292.
49. **Rodig, S. J., A. Shahsafaei, B. Li, and D. M. Dorfman.** 2005. The CD45 isoform B220 identifies select subsets of human B cells and B-cell lymphoproliferative disorders. Hum. Pathol. **36:**51–57.
50. **Rossi, M. I., K. L. Medina, K. Garrett, G. Kolar, P. C. Comp., L. D. Shultz, J. D. Capra, P. Wilson, A. Schipul, and P. W. Kincade.** 2001. Relatively normal human lymphopoiesis but rapid turnover of newly formed B cells in transplanted nonobese diabetic/SCID mice. J. Immunol. **167:**3033–3042.
51. **Sachsenberg, N., A. S. Perelson, S. Yerly, G. A. Schockmel, D. Leduc, B. Hirschel, and L. Perrin.** 1998. Turnover of CD4$^+$ and CD8$^+$ T lymphocytes in HIV-1 infection as measured by Ki-67 antigen. J. Exp. Med. **187:**1295–1303.
52. **Sawada, S., K. Gowrishankar, R. Kitamura, M. Suzuki, G. Suzuki, S. Tahara, and A. Koito.** 1998. Disturbed CD4$^+$ T cell homeostasis and in vitro HIV-1 susceptibility in transgenic mice expressing T cell line-tropic HIV-1 receptors. J. Exp. Med. **187:**1439–1449.
53. **Sekaly, R. P.** 2008. The failed HIV Merck vaccine study: a step back or a launching point for future vaccine development? J. Exp. Med. **205:**7–12.
54. **Shacklett, B. L.** 2008. Can the new humanized mouse model give HIV research a boost. PLoS Med. **5:**e13.
55. **Shearer, W. T., T. C. Quinn, P. LaRussa, J. F. Lew, L. Mofenson, S. Almy, K. Rich, E. Handelsman, C. Diaz, M. Pagano, V. Smeriglio, L. A. Kalish, et al.** 1997. Viral load and disease progression in infants infected with human immunodeficiency virus type 1. N. Engl. J. Med. **336:**1337–1342.
56. **Shultz, L. D., B. L. Lyons, L. M. Burzenski, B. Gott, X. Chen, S. Chaleff, M. Kotb, S. D. Gillies, M. King, J. Mangada, D. L. Greiner, and R. Handgretinger.** 2005. Human lymphoid and myeloid cell development in NOD/LtSz-scid IL2R gamma null mice engrafted with mobilized human hemopoietic stem cells. J. Immunol. **174:**6477–6489.
57. **Shultz, L. D., P. A. Schweitzer, S. W. Christianson, B. Gott, I. B. Schweitzer, B. Tennent, S. McKenna, L. Mobraaten, T. V. Rajan, D. L. Greiner, et al.** 1995. Multiple defects in innate and adaptive immunologic function in NOD/LtSz-scid mice. J. Immunol. **154:**180–191.
58. **Silvestri, G., M. Paiardini, I. Pandrea, M. M. Lederman, and D. L. Sodora.** 2007. Understanding the benign nature of SIV infection in natural hosts. J. Clin. Investig. **117:**3148–3154.
59. **Sun, Z., P. W. Denton, J. D. Estes, F. A. Othieno, B. L. Wei, A. K. Wege, M. W. Melkus, A. Padgett-Thomas, M. Zupancic, A. T. Haase, and J. V. Garcia.** 2007. Intrarectal transmission, systemic infection, and CD4$^+$ T cell depletion in humanized mice infected with HIV-1. J. Exp. Med. **204:**705–714.
60. **Tonomura, N., K. Habiro, A. Shimizu, M. Sykes, and Y.-G. Yang.** 2008. Antigen-specific human T-cell responses and T cell-dependent production of human antibodies in a humanized mouse model. Blood **111:**4293–4296.
61. **Traggiai, E., L. Chicha, L. Mazzucchelli, L. Bronz, J. C. Piffaretti, A. Lanzavecchia, and M. G. Manz.** 2004. Development of a human adaptive immune system in cord blood cell-transplanted mice. Science **304:**104–107.
62. **Trautmann, L., L. Janbazian, N. Chomont, E. A. Said, S. Gimmig, B. Bessette, M. R. Boulassel, E. Delwart, H. Sepulveda, R. S. Balderas, J. P. Routy, E. K. Haddad, and R. P. Sekaly.** 2006. Upregulation of PD-1 expression on HIV-specific CD8$^+$ T cells leads to reversible immune dysfunction. Nat. Med. **12:**1198–1202.

63. **VandeBerg, J. L., and S. M. Zola.** 2005. A unique biomedical resource at risk. Nature **437:**30–32.
64. **Velu, V., K. Titanji, B. Zhu, S. Husain, A. Pladevega, L. Lai, T. H. Vanderford, L. Chennareddi, G. Silvestri, G. J. Freeman, R. Ahmed, and R. R. Amara.** 2009. Enhancing SIV-specific immunity in vivo by PD-1 blockade. Nature **458:**206–210.
65. **Watanabe, S., K. Terashima, S. Ohta, S. Horibata, M. Yajima, Y. Shiozawa, M. Z. Dewan, Z. Yu, M. Ito, T. Morio, N. Shimizu, M. Honda, and N. Yamamoto.** 2007. Hematopoietic stem cell-engrafted NOD/SCID/IL2Rγ null mice develop human lymphoid systems and induce long-lasting HIV-1 infection with specific humoral immune responses. Blood **109:**212–218.
66. **Zaunders, J. J., G. R. Kaufmann, P. H. Cunningham, D. Smith, P. Grey, K. Suzuki, A. Carr, L. E. Goh, and D. A. Cooper.** 2001. Increased turnover of $CCR5^+$ and redistribution of $CCR5^-$ CD4 T lymphocytes during primary human immunodeficiency virus type 1 infection. J. Infect. Dis. **183:**736–743.
67. **Zhang, L., G. I. Kovalev, and L. Su.** 2007. HIV-1 infection and pathogenesis in a novel humanized mouse model. Blood **109:**2978–2981.